UNIVERSIDADE FEDERAL DO AMAZONAS
INSTITUTO DE CIÊNCIAS BIOLÓGICAS
PROGRAMA DE PÓS-GRADUAÇÃO
EM IMUNOLOGIA BÁSICA E APLICADA

ANTI-ARTHRITIC ACTIVITY OF DICLOFENAC LIPID-CORE NANOCAPSULES: A STEREOLOGICAL ANALYSIS APPROACH OF ARTHRITIS MODEL

NATHALIE MARTE UREÑA

MANAUS-AM, 2020

UNIVERSIDADE FEDERAL DO AMAZONAS
INSTITUTO DE CIÊNCIAS BIOLÓGICAS
PROGRAMA DE PÓS-GRADUAÇÃO
EM IMUNOLOGIA BÁSICA E APLICADA

NATHALIE MARTE UREÑA

ANTI-ARTHRITIC ACTIVITY OF DICLOFENAC LIPID-CORE NANOCAPSULES: A STEREOLOGICAL ANALYSIS APPROACH OF ARTHRITIS MODEL

A dissertation presented to the Postgraduate Program of Basic and Applied Immunology of the Federal University of Amazonas, as a prerequisite to obtaining the title of Master in Basic and Applied Immunology, in the area of Basic and Applied Immunology.

Advisor: Professor Antônio Luiz Ribeiro Boechat Lopes, MD, PhD.

Co-advisor: Professor Oscar Tadeu Ferreira da Costa, PhD.

MANAUS-AM, 2020

Ficha Catalográfica

Ficha catalográfica elaborada automaticamente de acordo com os dados fornecidos pelo(a) autor(a).

Ureña, Nathalie Marte
U75a Anti-arthritic Activity of Diclofenac lipid-core Nanocapsules: A Stereological Analysis Approach of Arthritis Model / Nathalie Marte Ureña. 2020
76 f.: il. color; 31 cm.

Orientador: Antônio Luiz Ribeiro Boechat Lopes
Coorientador: Oscar Tadeu Ferreira da Costa
Dissertação (Mestrado em Imunologia Básica e Aplicada) - Universidade Federal do Amazonas.

1. rheumatoid arthritis. 2. nanotechnology. 3. nanodrugs. 4. experimental model. 5. stereology. I. Lopes, Antônio Luiz Ribeiro Boechat II. Universidade Federal do Amazonas III. Título

UNIVERSIDADE FEDERAL DO AMAZONAS
INSTITUTO DE CIÊNCIAS BIOLÓGICAS
PROGRAMA DE PÓS-GRADUAÇÃO EM
IMUNOLOGIA BÁSICA E APLICADA

Ata do Exame de Defesa de Dissertação da aluna **NATHALIE MARTE UREÑA**, em 21 de fevereiro de 2020.

Aos vinte um dias do mês de fevereiro de dois mil e vinte, às dez horas, no Auditório do PPGIBA/UFAM, a aluna deste Programa **NATHALIE MARTE UREÑA** apresentou à banca examinadora a sua defesa de Mestrado intitulada: "Antiarthritic activity of diclofenac lipid-core nanocapsules: a stereological analysis approach". A banca examinadora, composta pelos seguintes membros: Professor Doutor Antonio Luiz Ribeiro Boechat Lopes (Presidente), Professora Doutora Maria Cristina dos Santos (Membro) e Professor Doutor José Fernando Marques Barcellos (Membro), após a apresentação e a arguição, decidiu: pela (X) aprovação ou pela ( ) reprovação de sua dissertação.

Professor Doutor **Antonio Luiz Ribeiro Boechat Lopes**
Presidente

Professora Doutora **Maria Cristina dos Santos**
Membro

Professor Doutor **José Fernando Marques Barcellos**
Membro

AGRADECIMENTOS

To my advisor Antonio Luiz Ribeiro Boecha, MD, PhD., for the advices, tips for the writing, for all the knwoledge he gave, and for the patience he always had.

To my co-advisor Oscar Tadeo Ferreira da Costa, PhD., for the help and teacheings on the laboratory process, for the advices and patience.

To Lene, for helping me with the procedures in the laboratory.

To my laboratory colegues, Vanda e Violeta, for their partnership and help when I needed.

To the professor Jose Fernando Marques, PhD., for helping with the digitalization of the microscopic sheets.

To the Postgraduate Program of Basic and Applied Immunology for the extension of deadlines.

To the Program of Aliaces fort he Education and Training -PAEC/OEA for the opportunity to come to Manaus to do my masters degree and to CAPES for the granting of the scholarship.

To my friends in Manaus for the partnership, patience and support.

To my family in Republica Dominica, for all the love and support through these years.

RESUMO

A artrite reumatóide (AR) é uma doença auto-imune, conhecida pela inflamação da sinóvia, principalmente nas pequenas articulações das mãos e os pes. A progressão da AR leva à perda da função das articulações e, se não tratada, à deformidade das articulações afetadas. A principal causa da AR ainda é desconhecida, mas alguns mecanismos de patogênese foram identificados, como a expressão do antígeno leucocitário humano HLA-DR4, linfócitos T auto-antígenos e auto-anticorpos expressos pelos linfócitos B. Este mecanismo é o alvo do tratamento. Os produtos farmacêuticos atuais usados para o tratamento da AR são medicamentos anti-reumáticos modificadores de doença (DMARDs), DMARDs biológicos e anti-inflamatórios não esteroides (AINEs). Todos esses produtos farmacêuticos causam toxicidade quando usados por um longo período de tempo e têm grandes efeitos adversos nos pacientes. Os efeitos adversos são devidos à baixa especificidade que eles têm para os tecidos inflamados. Por esse motivo, os pesquisadores estão começando a testar nanoformulações para tratamento. Nanodrogas ou nanofármacos são medicamentos encapsulados em um tamanho em nanômetros. Essa conformação fornece propriedades únicas para a administração específica de medicamentos em locais específicos, para evitar a degradação por enzimas e a liberação sustentada do medicamento. Os nanofarmacêuticos demonstraram melhor capacidade anti-inflamatória, imunomodulação aprimorada e menores taxas de progressão da doença. A importância de encontrar um melhor tratamento para a AR levou a este projeto. Nosso objetivo é avaliar a atividade de uma nanocápsula lipídica de diclofenaco em um modelo experimental de artrite induzida por adjuvante, utilizando análise estereológica. Através da geração de seções seriais das patas de ratos artríticos, aplicaremos análises morfológicos quantitativos para medir o volume, a densidade e a contagem de perfis celulares dos componentes das articulações. A avaliação será centrada na articulação metatarso-falangeal do segundo dígito. Observando mudanças na cartilagem articular, osso, membrana sinovial e espaço sinovial, avaliaremos a atividade anti-inflamatória do nanofarmacêutico. Medindo se a nanocápsula preservou a articulação.

Palavras chaves: artrite reumatoide, nanotecnologia, nanodrogas, modelão experimental, estereologia.

ABSTRACT

Rheumatoid Arthritis (RA) is an autoimmune disease, known for inflammation of the synovium in small joints that causes pain and stiffness. Some of the mechanisms of pathogenesis are auto-antigenic T lymphocytes and auto-antibodies expressed by B lymphocytes. These mechanisms are the target for treatment. The current pharmaceuticals used for the treatment of RA are Disease-Modifying Anti-Rheumatic Drugs (DMARDs), Biologic DMARD and Non-steroidal Anti-inflammatory Drugs (NSAIDs). All of these pharmaceuticals cause toxicity when used for a long period of time and have major adverse effects on the patients due to their low specificity for inflamed tissue. For this reason, researchers are beginning to test nanoformulations for treatment. Nanodrugs or nanopharmaceuticals are medications encapsulated in a nanoscale size. This conformation gives them unique properties for specific drug delivery at targeted sites, avoidance of degradation by enzymes and sustained release of the drug. Nanopharmaceuticals have demonstrated better anti-inflammatory capacity, enhanced immunomodulation and lower rates of progression of the disease. Our objective was to evaluate the activity of a Lipid core nanocapsule of Diclofenac (DIC-LNC) in an experimental model of adjuvant-induced arthritis, using stereological analysis. We applied quantitative morphological analysis to measure the volume, density and cellular profile count of the metatarsophalangeal articulation of the second digit. Our results demonstrated that DIC-LNC managed to reduce the volume of the joint in a more effective way than the Diclofenac solution. DIC-LNC preserved the synovial space and diminished synovitis of the arthritic joints. Our results suggest that Diclofenac lipid-core nanocapsules are effective at reducing joint inflammation.

Keywords: rheumatoid arthritis, nanotechnology, nanodrugs, experimental model, stereology.

LIST OF FIGURES

LIST OF TABLES

LIST OF ACRONYMS

ACPA Anti Citrullinated Protein Antibody

Ag Silver

ALP Alkaline Phosphatase

ALT Alanine Transaminase

AST Aspartate Transaminase or Aspartate Aminotransferase

Au Gold

BUN Blood Urea Nitrogen

CAIA Collagen Antibody Induced Arthritis

CFA Complete Freund's Adjuvant

CH Chitosan

COX-2 Ciclooxigenase 2

CRE Creatinine

CT Computed Tomography

CTX-II C-terminal Telopeptide Type II Collagen

CU Curcumin

DEX Dexamethasone

DMARDs Disease-Modifying Anti-rheumatic Drugs

FA Folic Acid

FRβ Folate Receptor beta

HA Hyaluronic Acid

HLA Human Leukocyte Antigen

IFN-y Interferon Gamma

IL-1α Interleukin one alpha

IL-1β Interleukin 1 beta

IL-6 Interleukin 6

IL-10 Interleukin 10

IL-17 Interleukin 17

LCN Lipid Core Nanocapsules

LPS Lipopolysaccharide

LX Lornoxicam

MMPs Metalloproteinases

MRT Mean Residence Time

MTT 3-(4,5-dimethylthiazol-2-yl)-2,5-diphenyltetrazolium bromide

MTX Methotrexate

NF-κB Nuclear Factor kappa beta

NSAIDs Non-steroidal Anti-inflammatory Drugs

OC Osteocalcin

OD Optical Density

PC Phosphatidylcholine

PCADK Poly Cyclohexane-1,4-diyl acetone Dimethylene ketal

PCL Polycaprolactone

PD Prednisolone

PEG Polyethylene Glycol

PEI Polyethylenimine

PG Prostaglandine

PGA Poly-γ-Glutamic Acid

PGE2 Prostaglandin E2

PLA Poly-l-Lactic Acid

PVA Polyvinyl Alcohol

RA Rheumatoid Arthritis

RF Rheumatoid Factor

siRNA Small Interfering RNA

SLN Solid Lipid Nanoparticles

TDD Transdermal Delivery

TLR-2 Toll like receptor 2

TLR-4 Toll like receptor 4

TNF-α Tumor Necrosis Factor alpha

TP Triptolide

LIST OF SYMBOLS

α – alpha

β – beta

κ- kappa

γ - gamma

Σ – sum

V - absolute volume

Vv - volume’s density of a component

Sv - surface density

1. INTRODUCTION

Rheumatoid arthritis (RA) is a chronic autoimmune disease with an incidence rate of 25-50 patients in each 100,000 population (UHLIG; MOE; KVIEN, 2014). RA starts primarily affecting the join. The affected patients refer symptoms of pain, swelling, and stiffness of small joints of hands and feet. Articular inflammation can be presented in an oligo or polyarticular pattern that progresses to deformation of the joints (GULATI; FARAH; MOUYIS, 2018).

The specific cause of RA is still unknown, but some genetic and environmental factors are related to the onset of the disease (MCINNES; SCHETT, 2007). The genetic expression of one allele of HLA-DR4, has been linked to the pathogenesis of RA and denominated the “susceptibility epitope” since 70% of RA patients express this allele (FIRESTEIN; MCINNES, 2017).

HLA-DR4 is linked to the citrullinated autoantigen presentation to autoreactive T cells allowing their activation and a specific Th1 and Th17 response at the synovial tissue (RAYCHAUDHURI et al., 2012). These reactions elicit the production of autoantibodies by B cells. Rheumatoid Factor (FA) and anti-citrullinated peptide auto-antibodies (ACPA) promote the production of TNF-α by the macrophage-like synovial cells, which then stimulate more inflammation in the joint tissue and, together with IL-1 and IL6, promote bone degradation (DAYER; CHOY, 2010). This reaction begins a cycle of activated innate and adaptive immune cells that destroy the articulation, causing the signs and symptoms of the patients (CHOY, 2012). These known mechanisms are the key targets for treating Rheumatoid Arthritis.

The current treatment for RA is based on the use of Disease-Modifying Anti-Rheumatic Drugs (DMARDs). These pharmaceuticals have shown the capacity to reduce inflammation and slow down the progression of RA (WENG et al., 2010).

DMARDs include pharmaceuticals like methotrexate, leflunomide, hydroxychloroquine, and sulfasalazine. All of them inhibit a specific inflammation mechanism, making a better treatment and improving medical outcomes when used in combination (MA; KINGSLEY; SCOTT, 2009). When the use of DMARDs fails, the next step for treatment is the implementation of Biologic DMARDs. Both biologic or synthetic DMARDs target specific molecules that are involved in the pathogenesis of RA, like TNF-α and IL-6 or cytokine receptor signaling pathway (STATKUTE; RUDERMAN, 2010; EMERY et al., 2008). Biologics are usually prescribed as monotherapy, but patients have shown a better response when they receive the combination of Biologics with methotrexate (FC et al., 2006).

Adding to this combined therapy, the prescription of Non-steroidal anti-inflammatory Drugs (NSAIDs) is used to manage pain sensation on RA patients. It is interesting to note that even patients using optimized therapeutic schemes are expressing high levels of cyclooxygenase enzymes at synovial tissues (KOROTKOVA; JAKOBSSON, 2014).

NSAIDs have an antipyretic, anti-inflammatory and analgesic effect, through the inhibition of cyclooxygenase (COX) (KROENKE; KREBS; BAIR, 2009). Most commonly used NSAIDs are diclofenac, ibuprofen and naproxen, but these medications are associated with serious gastrointestinal side effects and need to be in co-therapy with a proton pump inhibitor (PPI) (HUNT et al., 2009).

The gastrointestinal side effects related to NSAIDs causes the death of approximately 3500 to 16,500 patients per year (VAN DE LAAR, 2012). Moreover, selective COX-2 inhibitors like celecoxib or valdecoxib showed a reduction in gastrointestinal side effects, but are linked to increased cardiovascular risk along with the conventional NSAIDs (TRELLE et al., 2011). This is why the use of NSAIDs is recommended in minimum doses and for a short period of time.

As a solution to this problem comes the implementation of nanotechnology. This branch of science develops nanoscale formulations with a specific drug delivery system (GOUVEIA et al., 2015).

Nanotechnology offers formulations of nanomaterials that encapsulate the drug and deliver it into the site of inflammation (HOBSON, 2011). Nanopharmaceuticals are formulations that can have a size range between 1 to 100 nanometers (nm). Such small sizes give the nanomaterials distinctive chemical, biological and physical characteristics because the electrons that compose the structure have a limited oscillated capacity; developing unique optical, electric and magnetic properties (WEISSIG; PETTINGER; MURDOCK, 2014).

The advances in structure give additional properties to the active drug. Many studies have been made testing nanoformulations for the treatment of RA (ZHANG et al., 2018b; DOLATI et al., 2016; PHAM, 2011; NOGUEIRA et al., 2016; GHARAGOZLOO; MAJEWSKI; FOLDVARI, 2015). These formulations are demonstrating an enhanced anti-inflammatory and immunomodulatory activity at animal and cell experiments, however, there are no clinical trials registered to evaluate these effects in humans at the present moment.

The field of study for RA also implements the use of experimental models of arthritis, such as Collagen-induced Arthritis (CIA) (BRAND; LATHAM; ROSLONIEC, 2007), Adjuvant-induced Arthritis (AIA) (ASQUITH et al., 2009) and transgenic models that have genetic manipulations for specific receptors or cytokines (LI; SCHWARZ, 2003). These animal models mimic aspects of the disease which help to understand some of the mechanisms and contribute to the development of new treatments, without ever fully resembling human RA. The use of experimental models has introduced the application of stereological analysis in the field of study for RA.

Stereology is a morphological quantitative tool that helps analyze anatomic information of a three-dimensional structure, based on the quantitative analysis of two-dimensional images (GUNDERSEN et al., 2009). It is described as “unbiased stereology”, referring to the possibility of assertive quantitative analysis with minimum or without bias. This technique helps calculate measures like volume and density, through the counting of structures of the organ in the study (KRISTENSEN et al., 2008).

Stereology requires making sections with a microtome, of a geometrical structure or organ into 2D plane series. This transformation from 3D to 2D planes will vary the size, shape and frequency of profiles that are inside the geometrical structure. Stereology provides efficient tools to estimate volume, density, superficial area, length and number of objects (profiles) within an organ. After the 2D sections are made, geometric probes (grids) are imposed over the sections and the interactions or intersections between the grid and the structural features are counted to obtain precise measures of volume, density or superficial area (BOYCE et al., 2010).

Furthermore, stereology is capable of counting cellular profiles that are present in a sample. This is the *numerical density* in a plane. The counting is made through the implementation of a “counting frame” in the area of interest. This frame is made by two parallel section planes with a known distance. The profile particles (Q) are taken into account only if they are inside the frame and not intersected by the “excluding edges”. This gives the number of profiles per area (GUNDERSEN et al., 2009). Stereology combines statistical sampling principles with geometrical analysis to obtain precise results.

The purpose of our project is to evaluate the activity of a Diclofenac lipid-core nanocapsule (DIC-LNC) in experimental model of arthritis, using stereological methods to make a quantitative analysis of morphological material of the arthritic animals. The present study is the last branch of a bigger project of our team, that aims to evaluate the anti-inflammatory activity of a diclofenac lipid core nanocapsule DIC-LNC. The first step of the whole project was to develop the lipid core nanocapsule. The DIC-LNC was prepared at Laboratório de Nanotecnologia Farmacêutica of Universidade Federal do Rio Grande do Sul. The second step was to evaluate the anti-arthritic effect of diclofenac lipid core nanocapsules to control inflammation and joint damage on adjuvant-induced arthritis (AIA) model.

The last step of the study is our present project, the evaluation of the DIC-LNC activity through stereological analysis. We hypothesized that the DIC-LNC will have an anti-arthritic effect on the joints. DIC-LNC will preserved the synovial space and chondrocytes of the joint and will reduce the synovial inflammation. To determine the action that the

nanocapsule had on the arthritic articulations, we apply quantitative stereological methods to obtain quality results with minor bias. We calculated total volume, density, surface area and cellular profile count. These parameters gave us an insight into the effect that the DIC-LNC has arthritic joints.

CHAPTER 1- Review Article
Nanoformulations for Treatment of Rheumatoid Arthritis

ABSTRACT

Rheumatoid Arthritis (RA) is a chronic inflammatory autoimmune disease that begins with damage to the joints. This disease affects 1% of the world population. RA is characterized for inflammation of the synovium, immune cell infiltration, degradation of the cartilage and bone of the affected articulation that leads to loss of function. The treatment for this disease includes non-steroidal anti-inflammatory drugs (NSAIDs), glucocorticoids, disease-modifying antirheumatic drugs (DMARDs) and many more immune modulators. But these treatments have not been successful in the cure of RA, due to the many side effects that they cause. Another method that has been applied for the treatment of RA is the use of Natural or Traditional medicine. Traditional medicine applies plants extracts for their known therapeutic effect, to treat a certain symptom or disease. Generally, natural compounds of plant extracts have low solubility in the body and large amounts of them can be toxic to various organs of the body. These current drugs used to treat Rheumatoid Arthritis, have poor selectivity for inflamed tissue, making them easily absorbed by not inflamed tissue and organs, leading to toxicity. This is why Nanopharmacology has gained interest in the researcher that studies RA. Nanopharmacology formulates encapsulated nanoscale drugs that offer specific targeting for tissue, protection of the drugs inside the nanostructure, avoiding the degradation of the active compound and providing sustained drug activity. Furthermore, nanopharmacology enhances the selectivity of the drug in the nanostructure by adding specific ligands addressed to inflammatory cells. All of these advantages offer a possible solution for the treatment of RA. In this mini-review, we aim to provide some of the latest work that has been made using nanomaterials on an experimental model of arthritis. Merging the use of western medicine and Traditional medicine with nanotechnology.

Keywords: Rheumatoid arthritis, experimental model, nanodrugs, nanopharmacology, natural medicine.

1. Introduction

Rheumatoid Arthritis (RA) is a chronic synovial autoimmune disease, characterized by chronic inflammation of joints, which leads to loss of function and work disability, affecting 0.2 - 1% of the worldwide population (SMOLEN; ALETAHA; MCINNES, 2016; DINI et al., 2019). The joint degeneration process starts with asymptomatic inflammation of the synovium and gradually progresses to deformity and destruction of the articular cartilage and bone (ALETAHA et al., 2010a).

RA is one of the most prevalent autoimmune disease and its development is related to other comorbidities including cardiovascular disease, pulmonary, vascular, musculoskeletal and psychological disorders; all of these increasing the mortality rate of patients with Rheumatoid Arthritis (MCINNES; SCHETT, 2011). The specific cause of Rheumatoid Arthritis is still unknown. Studies have linked the development of RA with the human leukocyte antigen HLA-DRB1 locus, which has demonstrated susceptibility in patients. The allele HLA-DR4 is expressed in 70% of RA patients, for this reason, scientists give it the name of “susceptibility epitope” (ALMEIDA et al., 2011).

Other explanations for the cause of RA are molecular mimicry by the proteins of pathogens, T-cell senescence induced by HLA molecules and proinflammatory signaling non-related in response HLA and T cell activation (MCINNES, et al. 2011). Deciphering the specific cause of RA is key for treatment and prognosis. One key component of RA pathogenesis is the hyperplasia of the synovium of the joints, with major migration of immune cells that accumulate in the articular tissue and produce proinflammatory cytokines like TNF-α, IL-1β, IL-6 and IL-17 (SHARMA; BHAR; DEVI, 2017).

This cascade of cytokines induces the differentiation of B lymphocytes into plasma cells which then produce autoantibodies, known as anti-citrullinated protein antibody (ACPA) and rheumatoid factor (RF). The synthesis of ACPA, RF and proinflammatory cytokines lead to an autoreactive adaptive immune response and an ongoing cycle of destruction of the joint (SONG; KANG, 2009).

Not knowing the specific trigger of Rheumatoid Arthritis, makes it more difficult to find a cure. Current treatment includes non-steroidal anti-inflammatory drugs (NSAIDs), like aspirin and Diclofenac, which inhibit the activity of cyclooxygenase (COX), a known enzyme that induces inflammation. These drugs are used to treat the pain sensation of the patients. (CHAN et al., 2010).

Another group of pharmaceuticals is the glucocorticoids, like cortisone and prednisolone that inhibit the production of prostaglandins (PG) and tumor necrosis factor (TNF) helping on the reduction of inflammation of the joint tissue (FERREIRA; AHMED MOHAMED; EMERY, 2016). Finally, the disease-modifying antirheumatic drugs (DMARDs) and Biologic DMARDs, which include the anti-cancer drug Methotrexate, the immunosuppressant cyclosporin, anti-TNF-α monoclonal antibody adalimumab (LAMBERT, 2012).

DMARDs target specific molecules that intervene in the pathogenesis of RA, like proinflammatory cytokines and their receptors. The downside of these pharmaceuticals is the life-threatening adverse effects, like gastrointestinal and cardiovascular complications, impaired renal function, visual problems and increased risk of osteoporosis (BADER, 2012). All the adverse effects are due to the non-specific targeting for the inflamed tissue of these drugs leading to their systemic absorption.

This is when Nanopharmacology comes in discussion, offering medication in a nanosized particle with specific target release, avoiding all the adverse effects, minimizing the dosage of the drug with a sustained-release throughout the treatment (BONIFÁCIO et al., 2014). With these advantages, Nanopharmacology seems to be a promising way of treatment for Rheumatoid Arthritis. The aim of this review is to describe the recent work made applying nanopharmacology in the study of an experimental model of arthritis. Comparing western medicine pharmaceuticals and traditional medicine compounds with nanotechnology. We will emphasize the advantages that nanomedicine brings to this issue

2. Methodology

The references for this literature review were obtained from the following websites: *PubMed*, *ScienceDirect,* and Google Scholar. The timeline included for the search of the articles was between October 2000 and April 2019. The keywords for searching were: “rheumatoid arthritis”, “experimental model of arthritis”, “nanoparticles”, “nanotechnology”, “nanocarriers”, “herbal drug” and “traditional medicine”, "nanoemulsion", "nanocapsules".

3. Literature Review

3.1 A background in nanopharmacology

Nanopharmacology works with nanoscale materials that have improved physical, chemical and biological properties (ASHAI et al, 2012). These nanomaterials have an increased surface size due to their nanoscale dimension, characteristics that give them an enhanced reactivity and strength in *vivo* experimentation. Nanopharmacology develops nanodrugs or nanomedicines that run on a size range generally from 1-1000 nm and have a spherical shape. These nanoparticles have improved solubility by an increased surface-to-volume ratio (AHMED et al., 2016).

Nanopharmaceuticals provide a sustained release of the encapsulated drug, they reach the targeted tissue and deliver the pharmaceutical (FISSELL, 2013). These nanomedicines enhance the selectivity and effectiveness of treatment alleviating drug toxicity. All of this is possible due to two different mechanisms: passive and active targeting (KOTHAMASU et al., 2012).

Passive targeting is due to the enhanced vascular permeability at sites of inflammation. The intercellular union of endothelial cells at inflammation areas have gaps where the nanoscale drugs can go through and reach the inflammation site (BERTRAND et al., 2014). Active targeting is possible thanks to adhesion or specific ligands for target cell receptors to the nanostructured pharmaceutical. Another advantage is the encapsulation of the drug, that protects it from excessive metabolism by enzymes, proteins, and other cells. Providing a major quantity of the drug to the specific tissue (CHUANG et al., 2018).

3.1.1 Types of nanoformulations according to their structural components

Polymeric Nanoparticles

Polymeric nanoparticles are generally made out of PGA (poly-γ-glutamic acid), polyethylene glycol (PEG), polyvinyl alcohol (PVA), poly-l-lactic acid (PLA), polycaprolactone (PCL), or chitosan (CH). They are biodegradable, biocompatible and minimally immunogenic. Polymeric nanoparticles can be synthesized as nanocapsules (polymeric shell) or nanospheres (porous shell) (DUDICS et al., 2018).

Metal-oxide Nanoparticles

Metallic nanoparticles are usually made out of silver (Ag) or gold (Au). They have a higher surface area and larger pore sizes which gives them the ability of better drug encapsulation. The metal gives to the nanoparticle unique biodegradable characteristics, caused by the formation of labile bonds with the ligands (AHMED; ALJAEID, 2016).

Liposomes

Liposomes are vesicles with nanoscale-sized and spherical shape made out of a bilayer of biological phospholipids. A lipophilic drug can be transported dissolved in the bilayer of the liposomes (ALLEN; CULLIS, 2013).

Nanoemulsions

Nanoemulsions are an isotropic system, a diffusion of two non-miscible liquids, generally water and oil. This diffusion is stabilized by a surfactant that helps decrease the tension between the water phase and the oil phase. Their size ranges from 20-500 nm, they have high surface area and optical transparency (SINGH et al., 2017; JANAKIRAMAN et al., 2018).

Solid Lipid Nanoparticles

Solid Lipid Nanoparticles (SLN), combine the characteristics of nanoemulsions and polymeric nanoparticles. They are made of phospholipids, fatty acids, monoglycerides, diglycerides and triglycerides. As their name describes, these nanomaterials have a solid hydrophobic core surrounded by phospholipids. Their size ranges from 120-200 nm. SLN have the capacity to carry lipophilic and hydrophilic drugs (KUMAR et al., 2018; GESZKE-MORITZ; MORITZ, 2016).

Nanomicelles

Nanomicelles are composed of a monolayer of phospholipids. They are an amphipathic particle, with a hydrophobic core, for the encapsulation of hydrophobic drug, and a hydrophilic shell for better solubility. This junction of monomers ranges from 50-200 nm (VADLAPUDI; MITRA, 2013).

Nanocapsules

Nanocapsules have an internal core for the active materials and an external polymeric shell that protects the core from degradation. This is the reason why sometimes is described as polymeric nanoparticle. Nanocapsules can transport drugs in the form of liquid, solid or molecular dispersion. Their size ranges from 10-1000 nm. (BALE et al., 2016; WANG et al., 2016)

Lipid-core Nanocapsules

Lipid core nanocapsules are made out of triglycerides and sorbitan monostearate covered by a polymeric wall. The core is formed by a liquid lipid and a solid lipid. Lipid-core nanocapsules derive from Nanocapsules (FRANK et al., 2015)

Biomimetic Nanoparticles

They imitate the natural characteristics of cell particles and cell membranes. These nanomaterials have the benefits of synthetic nanoparticles and natural nanomaterials. They mimic natural mechanisms of the immune system to get to the inflammation area. Biomimetic nanoparticles can be: 1) Synthetic nanomaterials with a targeting ligand that imitates a cell membrane protein, 2) Nanoparticle coated with cell membrane or topdown

strategy or 3) Liposomes with cell membrane proteins. Whatever the structure, Biomimetic nanoparticles have enhanced selectivity for inflammatory areas making the delivery of the drug more accurate (JIN et al., 2018).

3.2 Nanopharmacology in experimental model of Arthritis

Many studies have been made regarding nanomedicine and the treatment of Rheumatoid Arthritis. Prabhu et al. demonstrated the anti-rheumatic effect that lipid nanovesicles loaded with methotrexate on adjuvant-induced arthritis induced rats, compared with the free solution of methotrexate (MTX). They observed a significant diminution of edema volume in the hind paws of rats treated with the PEGylated MTX liposomal formulation in comparison with the arthritis control group that did not receive any treatment. The highest anti-rheumatic efficacy was observed in the PEGylated MTX nanoformulation, followed by the chitosan-coated lipid vesicles and at last the conventional treatment with a free solution of MTX. When analysing the serum levels of hepatic proteins of each treatment group, SGOT and SGPT levels of the nanoformulations were significantly lower in comparison with treatment of MTX solution. Their results demonstrate the effectiveness that lipid vesicles have on the treatment of experimental arthritis (PRABHU et al., 2012).

Following the lipid nanostructure particles, a lipid nanoemulsion of methotrexate (LDE-MTX) was tested in rabbits to measure its anti-inflammatory activity on experimental arthritis. Mello et al. induced arthritis on New Zeland white rabbits with CFA. Their results showed a significant reduction of leukocytes count on the synovial fluid of the rabbits treated with LDE-MTX with doses of 0.25 and 0.5µmol/kg when compared with the control group that did not receive any treatment. Furthermore, the lipid nanoemulsion showed a better reduction of cytokines levels of IL-17 and IFN-y when compared with commercial MTX that did not altered cytokine levels of the synovial fluids (MELLO et al., 2013).

A few years later, studying the same drug (MTX), Boechat et al. compared the anti-inflammatory effects of methotrexate and lipid-core nanocapsules loaded with methotrexate (MTX-LNC), on a chronic animal model of arthritis in rats and in vitro cells, obtained from synovial fluid of RA patients. Analysing the edema volume of the hind paws, they observed similar results when comparing MTX-LNC with MTX, taking in

consideration that the dose of MTX inside the nanocapsule was 75% lower than the solution of MTX. The animal group treated with the loaded nanocapsules also presented significantly lower levels of proinflammatory cytokines TNFα and IL-1α. Also the CRP levels of the MTX-LNC group were lower in comparison with the solution of MTX. The in vitro experiments with the human synovial cells, the group that received loaded nanocapsules showed a reduction of the proinflammatory cytokines TNFα and IL-6 and lower levels of IFN-y and IL-17A. Demonstrating a better anti-inflammatory activity of methotrexate when administered in nanocapsules (BOECHAT et al., 2015).

In 2017 Zhao et al., published their work on polymeric lipid nanoparticles loaded with methotrexate (PPLNP/MTX) marked with folic acid (FA) ligand. The FA ligand was produced with the purpose to interact with the folate receptor (FRβ) of activated macrophages of the inflamed areas. The authors observed the lowest clinical score for the group treated with FA-PPLNPs/MTX, reaching on day 19 a score of 0.6. The nanoparticle with the folic acid ligand showed a significantly reduced paws thickness in comparison with the PPLNP/MTX and with the solution of MTX. The biochemical analysis showed a significant reduction of serum levels of TNF-α and IL-6 in comparison with MTX. Furthermore, on the in vitro tests with RAW246.7 cells they analyzed cell uptake of the nanoparticles with a rhodamine B fluorescent test. They observed that the activated macrophages that were treated with FA-PPLNPs/MTX showed higher intensity of rhodamine B, suggesting a better uptake of the nanoparticle due to the ligation of the FA ligand with the FRβ receptor (ZHAO et al., 2017).

Also targeting the folate receptor Duan et al., fabricated a liposome loaded with siRNA and MTX with a pegylated coating and folate ligand (F-siRML) to increase the selectivity of the nanoparticle. They used siRNA to silence the gene of NF-kB and enhance the anti-inflammatory activity of the MTX nanoparticle. The authors observed a significant reduction of paw thickness and arthritic score on the mice treated with F-siRML in comparison with siRML and free MTX. Also they observed a larger diminution of the inflammatory cytokines TNF-α and IL-1β. The team measured the lymphocyte count of the treated mice and observed no diminution of lymphocytes on the mice that received the F-siRML. On the in vitro test, they activated RAW246.7 cells with LPS and measured

through fluorescence the uptake of the FA nanoparticle in comparison with another nanoparticle that did not contain the FA ligand. They observed a sustained uptake of the FA loaded liposome by higher fluorescence. The results show the efficacy and selectivity that nanoformulations can offer for treatment, without causing side effects (DUAN; LI, 2018).

Following the line of targeting the folic acid receptor, Shi et al., tested the anti-inflammatory capacity of chitosan (CH) nanocarrier with folic acid ligands (FA), formulated with polyethylene glycol (PEG) and carrying siRNA (folate-PEG-CH-DEAE15/siRNA) to silence TNF-α gene. Their results presented a significant decrease of arthritic score and hind paw edema in the group of animals treated with folate-PEG-CH-DEAE15/siRNA when compared with the control group and CH-DEAE15/siRNA-TNFα. Via immunohistochemistry they observed a diminution on the concentrations of TNF-α in the synovium of mice. To analyze the degradation of cartilage and bone, they used the bone density test and serum levels of CTX-II (C-terminal telopeptide type II collagen), ALP (Alkaline phosphatase) and OC (osteocalcin). The group that received the folate chitosan nanoparticle showed better conservation of the cartilage and bone structures with lower levels of serum CTX-II (SHI et al., 2018).

Using NSAIDs therapeutics, one group studied the anti-inflammatory capacity of indomethacin loaded nanocapsules (IndOH-NC) on experimental model of arthritis. On the acute protocol of arthritis, they observed a major reduction of paw edema in the rats that received IndOH-NC compared with the solution of IndOH. With the chronic protocol of edema, the indomethacin nanocapsule also presented a marked reduction of paw edema. In the biochemical analysis the treatment with IndOH-NC showed a significant reduction of the serum levels of TNF-α, IL-6 and a significant increase of the anti-inflammatory cytokine IL-10. Finally the group analyzed the gastrointestinal lesional index (LI) of the arthritis group and observed the lowest LI on the group treated with IndOH-NC. Demonstrating the efficacy of the anti-inflammatory activity of the encapsulated drug and avoidance of adverse effects (BERNARDI et al., 2009).

Also applying NSAIDs, Nguyen et al, tested the transdermal drug delivery (TDD) capacity of a Diclofenac loaded lipid nanocarrier (DFC-LNC). They observed that particle size and

composition of lipids of the nanoparticles have major impacts on transdermal drug delivery. The amount of permeated drug after 24hrs of the application was higher with the nanocarrier that had a smaller size. Furthermore, these same small nanocarriers presented a more efficient reduction of paw edema, when compared with the solution of Diclofenac. Since nanoparticles have instant access to the skin with a better absorption rate, they obtained the strongest diminution on paw edema with these nanomedicines (NGUYEN et al., 2017).

Another NSAID used for the treatment of RA, is Lornoxicam (Lx), preferred by many because of its protective effect against RA (TAYAL, 2012). In 2017, Helmy et al.,published their work on lornoxicam loaded nanomicellar (Lx-NM) formulas on experimental model of RA. Analyzing the paw edema of the rats, they observed that the higher doses of Lx-NM produced a significant reduction of the edema volume in comparison with the low dose of Lx-NM. Furthermore, they observed that the nanomicellar formulation produced more reduction of the edema, than the free solution of Lx. Also, the use of Lx-NM significantly reduced the serum levels of TNF-α, IL-1β, PGE2 and NF-kβ. The treatment with the nanomicellar formula showed a significant decrease in levels of malondialdehyde and nitric oxide. Demonstrating a better efficacy of the drug in the nanoparticle presentation (HELMY et al., 2017).

Using polymeric nanoparticles, Shao et al., tested the capacity of rapamycin to regulate the immune response in RA mice model and in vitro tests. The in vitro test with the rapamycin/NP showed a downregulation on the activation markers CD80+ and CD40+ of dendritic cells. Also, the production of proinflammatory cytokines by macrophages was reduced when treated with rapamycin/NP. All IL-6, TNF-α and IL-1β cytokines had a significant reduction compared with the empty nanoparticle. The results of the in vivo experiment showed that the rapamycin/NP caused a marked reduction in clinical score and diminution of serum levels of TNF-α and IL-6. Demonstrating an enhanced immune regulation by the drug presented on the nanoformulation (SHAO et al., 2017).

On the line of glucocorticoid therapy, Zhou et al., tested the efficacy of solid lipid nanoparticles (SLN) loaded with Prednisolone (PD) with hyaluronic acid (HA) as ligand to enhance specificity (HA-SLNs/PD), reduce the high doses and long term glucocorticoid

therapy. The authors observed that the arthritic score of mice treated with the coated nanoparticle was the lowest (mean score 1) in comparison with free prednisolone (mean score 2.9) and the uncoated nanoparticle (mean score 2). Also, the HA coated nanoparticle reduced joint swelling and erosion of the bone of the mice. Furthermore, the serum levels of proinflammatory cytokines (TNF-α, IL-1β, IL-6) were reduced on the mice treated with HA-SLN-PD. These results demonstrate efficacy and selectivity of the drug, when presented as a nanoparticle (ZHOU et al., 2018).

Merging the use of glucocorticoids and polymeric nanoparticles, Yu et al., formulated a lipid-polymer hybrid nanoparticle loaded with Dexamethasone (Dex). Using PCADK; Poly (cyclohexane-1,4-diyl acetone dimethylene ketal); egg phosphatidylcholine (egg PC) and polyethylenimine (PEI) with a coating of Hyaluronic acid (HA) for the structure of the nanoparticle. The rhodamine B test showed strong fluorescence in the cells that received HAPNPs/Dex nanoparticles in comparison with the nanoparticles that did not have HA. On the in vivo experiment, the authors observed a decrease in the clinical score of the rats treated with the hybrid nanoparticle (HAPNPs/Dex). The paw thickness of the rats treated with HAPNPs/Dex, was considerably lower compared with the other treatments. Also, the rats treated with HAPNPs/Dex showed better conservation of bone and cartilage structure with a reduced cell infiltration (YU et al., 2019).

These studies (**Table 1**) showed that the common drugs used for treating rheumatoid arthritis, have a better capacity of action when presented in any form of nanoparticle drug delivery system. Avoiding toxicity and adverse effects. The use of nanoparticles can also enhance the activity of other types of pharmaceuticals.

Table 1. List of pharmaceuticals and their nanoformulations on experimental model of Arthritis.

Drug/Agent	*Nanoformulation*	*Nanoparticle size*	*Compared treatment*	*Experimental model*	*in vitro Test*	*Effect on arthritic joint*	*Effect on blood, tissue and fluids*	*References*
Methotrexate	Lipid Nano vesicles 1)DSPC:MPEG DSE: CH (0.13 mg/kg i.v.) 2) DSPC: CH (0.13 g/kg i.v.)	1) 210 nm 2) 253 nm	Mtx solution 0.13 mg/kg i.v.	AIA	--	Diminution of paw edema volume (*P<0.01*) by the DSPC:MPEGDSE: CH	Decrease on serum levels of hepatic proteins SGOT and SGPT (*P<0.01*).	(PRABHU et al., 2012)
	Lipid Nanoemulsion LDE-MTX (0.0625, 0.125, 0.25 and 0.5 µmol/kg i.a.	60 nm	Mtx solution 0.5 µmol/kg i.a.	AIA	--	Decline of cell infiltrate on the synovial membrane.	Reduction of leukocytes count on the synovial fluid (*P=0.004*) and diminution of cytokines levels of IL-17 (*P = 0.05*) and IFN-y (*P = 0.05*)	(MELLO et al., 2013)
	Lipid-core Nanocapsule MTX-LNC (0.375 mg·kg-1)	175±17 nm	Mtx solution 1.5 mg·kg-1	AIA	Human mononuclear synovial cells	Diminution of paw edema similar to Mtx solution (P=0.951).	Lower levels of proinflammatory cytokines TNFα (*P=0.0114*), IL-1α (*P=0.778*) and CRP (*P=0.011*). *In vitro:* reduction of the proinflammatory cytokines TNFα and IL-6 (P=0.046 and P=0.033),	(BOECHAT et al., 2015)

							IFN-y (P=0.046) and IL-17A (P=0.006).	
	Polymeric lipid nanoparticle with Folic Acid ligand 1)PPLNP/MTX (257 µg/kg) 2)FA-PPLNPs/MTX (257 µg/kg)	1) 148.8 nm 2) 133.6 nm	MTX solution 0.5 mL	AIA	Activated RAW246.7 cells	FA-PPLNPs/MTX showed decrease of clinical score (score 0.6) and paw thickness (*P < 0.01*). Lower bone and cartilage erosion of the joint.	Reduction of serum levels of TNF-α (P< 0.001) and IL-6 (P< 0.01) *In vitro:* Higher uptake of the nanoparticle by better interaction of the FRβ receptor	(ZHAO et al., 2017)
	Calcium phosphate/liposome-based hybrid nanocarrier loaded with siRNA and Folic Acid ligand (F-siRML)	170 nm	MTX solution 0.6 mg/kg	CIA	Activated RAW246.7 cells	Reduction of paw thickness and arthritic score (*P< 0.001*)	Diminution of the inflammatory cytokines TNF-α (< 15 pg/mL) and IL-1β (< 10 pg/mL) *In vitro*: Increase internalization of the nanoparticle with better interplay of ligand and receptor activity.	(DUAN; LI, 2018)
siRNA-TNF- α	Polymeric nanocarrier of Chitosan with		Naocarrier without				Diminution on the concentrations of TNF-α in the synovium	

	Folic Acid ligands (folate-PEG-CH-DEAE15/siRNA, 50 µg siRNA)	233±21 nm	folic acid ligands (CH-DEAE15/siRNA-TNFα, size 259±3 nm)	CAIA	Hela cells (cell viability)	Decrease of inflammation and arthritic score (*P<0.05*)	(*P<0.05*), low serum levels of CTX-II (P<0.05). *In vitro:* 89-97% cell viability with both nanoparticles.	(SHI et al., 2018)
Indomethacin	Nanocapsule (IndOH-NC, 1 mg·kg-1 i.p.)	240 nm	Indomethacin (IndOH) solution (1 mg·kg-1 i.p.)	1)Carrageenan 2)AIA	--	1)Carrageenan: reduction of paw edema (44±7%, P < 0.05) 2)AIA: reduction of paw edema (33 ±4%, P<0.05)	2) AIA: Reduction of serum levels of TNF-**α** (P<0.05), IL-6 (P<0.01) and increase of IL-10 (P<0.001). Low gastrointestinal lesional index (LI) (*P<0.001*)	(BERNARDI et at., 2009)
Diclofenac	Nanostructure Lipid Carrier (DFC-NLC) NLC1: 0.5% DFC NLC2: 0.4% DFC NLC3: 0.2% DFC	NLC1: 54.38 ± 1.54 nm, NLC2: 126.67 ± 1.21 nm, NLC3: 92.75 ± 0.82 nm (all transdermal)	(Voltaren Emulgel; Vol) transdermal	Carrageenan	--	Reduction of edema with all nanocarries (*P<0.01*). NLC1 presented 72.2% inhibition of inflammation	Better transdermal drug permeation with NLC1 (153.3%).	(NGUYEN et al., 2017)
	Nanomicelle		1)Lornoxicam (Lx)	1)Carrageenan		1)Carrageenan: higher doses of Lx-NM cause		

Lornoxicam	(Lx-NM) 1)Doses 0.325, 0.65 and 1.3 mg/kg, i.p. 2)Dose 0.325 mg/kg i.p.	169.45 nm	solution (1.3 mg/kg, i.p.) 2)Lx solution (0.325 mg/kg i.p.)	2)AIA	--	reduction of paw edema (*p <0.001*) 2)AIA: reduction of paw edema (*p<0.001*)	2)AIA: reduced the serum levels of TNF-α, IL-1β, PGE2 and NF-kβ (p<0.001)	(HELMY et al., 2017)
Rapamycin	Polymeric nanoparticle (rapamycin/NP, 135 µg)	165±35 nm	Empty nanoparticle (NP, 1 mg)	CIA	1)Mice spleen DC 2)Mice bone marrow macrophages	Reduction on the clinical score (mean score 7)	Diminution of serum levels of TNF-α and IL-6 (P<0.05). *In vitro*: DC: downregulation on the activation markers CD80+ and CD40+ (P<0.05). Macrophages: reduction on cytokine production IL-6, TNF-α and IL-1β (P<0.05)	(SHAO et al., 2017)
Prednisolone	Solid Lipid Nanoparticle coated with Hyaluronic Acid 1)HA-SLNs/PD (15 mg PD/kg)	1) 166.86 ± 1.25 nm 2) 147.8 ± 1.46 nm	Prednisolone (PD) solution (15 mg PD/kg)	CIA	RAW264.7 cells	Low arthritic score (mean score 1)	HA-SLNs/PD presented longer periods on plasma (29 µg/mL) and the joints. Serum levels of proinflammatory cytokines (TNF-α, IL-1β, IL-6) were reduced (*p < 0.05*)	(ZHOU et al., 2018)

	2)SLNs/PD (15 mg PD/kg)						*In vitro:* higher uptake of HA-SLNs/PD than SLN/PD (*p<0.05*)	
Dexamethasone	Acid sensitive Polymeric Nanoparticle 1)HAPNPs/Dex 2)HANPs/Dex 3)PNPs/Dex	1)150 nm 2)not shown 3)not shown	Dexamethasone (Dex) solution (5 mg/kg)	AIA	RAW 264.7 cells	Low clinical score presented by the HAPNP/Dex (*p<0.001*) and reduced paw thickness (*p<0.001)*	Conservation of bone and cartilage structure with a reduced cell infiltration. Low levels of serum TNF-α (*p<0.01*) and IL-6 (*p<0.001*) *In vitro:* higher uptake of HAPNPs/Dex	(YU et al., 2019)

The *in vitro* release tests of the papers were not taken in consideration for this table. **Abbreviations**: AIA, adjuvant induced arthritis; CIA, collagen induced arthritis; CAIA, collagen antibody induced arthritis; SGOT, aspartate aminotransferase; SGPT, serum glutamic pyruvic transaminase; INF-y, interferon gamma; TNF- α, tumor necrosis factor alpha; PGE2 prostaglandin e two; NF-Kb, nuclear factor kappa b; CRP, c-reactive protein; IL-1β, interleukin 1 beta; IL-1 interleukin 1; IL-6, interleukin 6; IL-10, interleukin 10; IL-17 interleukin 17.

3.3 Traditional Medicine meets Nanotechnology

Natural plant extracts are the basis of many pharmaceutical drugs and can have their therapeutic effects enhanced when applied with nanomaterials (STROHL, 2000). Usually these plant extracts have low bioavailability because they are easily degraded and nanoparticles provide the structure to keep the active principle from being degraded by enzymes. This is why both therapeutic branches, traditional medicine and nanopharmacology, have merged to provide enhanced natural medications (DEVI; JAIN; VALLI, 2010).

Traditional medicine applies the use of plant extracts to treat diseases. Many plants have been attributed with the capacity to treat Rheumatoid Arthritis (CAMERON et al., 2009). In Chinese traditional medicine is well known the use of Tripterygium wilfordii plant to treat inflammatory and autoimmune diseases (MATTA et al., 2009). Triptolide (TP), is a diterpenoid epoxide, present in this Chinese plant. This chemical compound has proven to have the immunosuppressive capacity and protective activity towards inflamed joints in RA. But the serious side effects that Triptolide (TP) causes, restrain its use (LI et al., 2017).

To prove the medicinal capacity of TP, Zhang et al. made a polymeric nanocarrier system containing Triptolide (PAT) and tested it on arthritic transgenic mice (TNF-α transgenic). Evaluating through near-infrared range with ICG, the authors observed that 24hrs after the administration, PAT tended to accumulate more at the inflamed joints, remained positive at 48hrs and was completely cleared after 80hrs. For cytotoxicity the authors made kidney and liver function tests. Treatment with PAT presented lower damage to the liver and kidneys (ALT: 81.58±14.12 mmol/L; AST: 38.58±18.38 mmol/L; CRE: 175.36±35.76 mmol/L; BUN: 7.84±1.30 mmol/L). In addition, the TP loaded nanoparticle showed a reduction of inflammation on synovium, less cartilage loss and reduced bone erosion on the knees and ankles of the treated mice. These results demonstrate the efficacy and reduced toxicity that the implementation of nanoparticles offer (ZHANG et al., 2018).

More recently, Gu et al.made a study using transdermal drug delivery (TDD) of Triptolide lipid nanocarriers (TPL-NLCs), to the inflamed joints of CFA's arthritic rats. The authors made in vitro analysis to evaluate drug permeation with Franz diffusion cells method, using excised rat skin. The penetration rate of TPL-NLC was 73.51 ± 17.29 μg/cm2 and for the nanoemulsion 23.94 ± 0.78 μg/cm2. On the in vivo experiment, the team analyzed the concentration of the Triptolide loaded lipid nanocarrier in the skin and plasma of the rats with a synchronous microdialysis system. The scientists observed a high mean residence time (MRT) on the plasma of the nanocarrier (20.06h) and a longer half-life in the blood (12.2 fold). Their results demonstrated a diminution in joint edema of the knees of the animals treated with TPL-NLC. Also the nanocarrier showed diminution on the expression of proinflammatory cytokines TNF-α, IL-1β and IL-6 of the joint fluids. Presenting a promising treatment for inflammation-related to rheumatoid arthritis (GU et al., 2019).

Another plant extract known for its medicinal properties is *Curcuma longa* L. (Zingiberaceae) or Curcumin. Curcumin is found in Turmeric, an ancient Asian spice. One of its active components is curcuminoid, recognized for anti-inflammatory, antibacterial, antiviral and antifungal effects (JURENKA, 2009). The anti-inflammatory properties of curcumin come from its ability to modulate some pro-inflammatory compounds like TNF-α, IL-1β, IL-6, NF-kB, COX-2 and others (MOGHADAMTOUSI et al., 2014).

In 2018, Fan et al., made a study using curcumin as a treatment for arthritic rats. They formulated a nanomicelle composed of Hyaluronic acid (HA) and Curcumin (Cur), and tested the anti-inflammatory and joint lubrication capacity of this nanomaterial. The in vitro tests showed elevated proliferation of chondrocytes for all the concentrations of nanomicelles tested. The authors analyzed the edema of the ankle with the CT energy spectrum and observed that the group of rats treated with the nanomicelle had a major diminution of edema (30%) in comparison with the other treatments. When evaluating the ankle joint with Multiple planar reconstruction photographs of CT, the HA/Cur nanomicelle group presented the less blurred articular surfaces with no swelling of the soft tissues. The histological analysis of the ankle joints revealed no evidence of inflammation or cartilage damage in the group treated with the nanomicelle. Finally, the authors tested the lubrication status of the joints with a UMT-2MT tribometer in a ball-on-plate contact

configuration. Here the HA/Cu group presented the lowest friction coefficient (~0.03) in comparison with the other treatments. Suggesting a better function of the knee articulation (FAN et al., 2018).

In Pakistan, traditional medicine recognizes the anti-inflammatory and antioxidative capacity of the cactus Opuntia dillen (MAHMOOD, MAHMOOD, TABASSUM, 2018). This plant has been used to treat asthma, gastric ulcers and diabetes. Its therapeutic effects are conferred by the two major compounds α-pyrones opuntiol and opuntioside. These two have demonstrated anti-inflammatory and antinociceptive effects (SIDDIQUI et al., 2016).

Roome et al. studied the antirheumatic capacity of opuntiol (OP) and opuntioside (OPG) in silver and gold nanoparticle formulations (OP-AgNPs/ OP-AuNPs). They tested the metallic nanoparticles in an experimental model of arthritis with Wistar rats. Also, the authors target mRNA expression of TLR-2, TLR-4, IL-1β and TNF-α. The results demonstrated a greater diminution of the arthritic score (score 1), in the groups receiving the metallic nanoparticles at a dose of 1 and 3 mg/kg. Furthermore, OP-AgNPs and OP-AuNPs reduced paw inflammation on >40% compared to the non-treated rats. Radiographic analysis showed minor edema of the soft tissue and mild erosion of the bone in the presence of opuntioside nanoparticles. On the histological analysis, the gold and silver nanoparticles showed better conservation of the joint tissue with a diminution of inflammatory cell infiltration. Furthermore, in rat spleen tissue the expression of TLRs was diminished from 65-80% in the presence of metallic nanoparticles. (ROOME et al., 2019).

These studies are summarized in **Table 2**

4. Conclusion

As the number of patients diagnosed with Rheumatoid Arthritis grows, the need for an effective treatment turns urgent. Many pharmaceuticals have been created for this purpose, but their poor specificity for tissue makes them prominent to serious side effects. Studies with nanopharmaceuticals are demonstrating a better range of action on treating

diseases. With their high specificity for inflamed tissue, they provide target delivery and sustained release of the drug. Encapsulating the pharmaceuticals or plant extracts, in nanomaterials avoids the dissemination of the drugs through the whole system, minimizing the side effects that these could cause. Nanopharmacology is a promising field for the treatment of Rheumatoid Arthritis. Even though the results presented with these nanomaterials seemed to be nonharmful for *in vivo* and *in vitro* experiments, these scenarios could not represent the systemic reactions that nanoformulations could have on humans. For this reason, more studies need to be conducted.

Disclosure

This article is unpublished and the authors report no conflict of interest during the evaluation.

Table 2. List of Nanoformulations loaded with natural compounds in the use of experimental model of Arthritis.

Plant Name	*Bioactive Compound*	*Nanoformulation*	*Size (nm)*	*Compared treatment*	*Experimental Model*	*In vitro test*	*Effect on arthritic articulation*	*Effect on blood, fluids and tissue*	*References*
Tripterygium wilfordii	Triptolide	Polymeric Nanoparticle (PAT) (0.15 mg/kg TP)	79±18	Triptolide (TP) solution (0.15 mg/kg, i.v.)	TNF- α Transgenic mice	RAW246.7 cells	Higher absorption of the nanoparticle on inflamed joints. Conservation of bone and cartilage of the joint.	Low damage to the liver and kidneys. *In vitro*: high cellular viability (*P<0.05*) and low apoptosis rate 7.2%	(ZHANG et al., 2018)
		Lipid Nanocarrier (TPL-NLCs) (90 mg/kg)	179.0 ± 0.286	Diclofenac sodium gel (25 mg/kg)	AIA	Franz diffusion cells method with excised rat skin	Diminution in joint edema of the knees (*P<0.05*)	Elevated penetration rate 73.51 ± 17.29 μg/cm2. High MRT on plasma 20.06h and longer half life in blood (12.2 fold). Reduced levels TNF-α, IL-1β and IL-6 (*P<0.05*)	(GU et al., 2019)

Curcuma alonga L. (Curcumin)	Curcuminoid	Nanomicelle (HA/Cur) (336 μg/mL)	164	Curcuminoid solution (Cur, 100 μL)	AIA	Bovine chondrocytes	Diminution of edema (30%, $p<0.05$), conservation of bone and cartilage of the joint.	Diminution of TNF-α , IL-1 ($p<0.05$) and liver proteins (AST,ALT, ALP). Friction coefficient (~0.03) *In vitro*: elevated proliferation of chondrocytes with ~3.7 absorbance.	(FAN et al., 2018)
Opuntia dilleni	Opuntiol Opuntioside	Metallic Nanoparticles (OP-AgNPs/ OP-AuNPs) (10 mg/kg)	5-7	1)Opuntiol (OP) and opuntioside (OPG) solution (100 mg/kg) 2) Dexa 0.5 mg/kg) 3)Indo 5 mg/kg)	AIA	Rat splenocytes	Diminution of arthritic score (score 1) and reduced paw inflammation on >40%.	Conservation of the joint tissue with diminution of inflammatory cell infiltration. Reduction on the expretion of TLRs 65-80%. In vitro: low levels of IL-1β and	(ROOME et al., 2019)

								TNF-**α** (*p<0.001*)	

Abbreviations: AIA, adjuvant induced arthritis; TNF- α, tumor necrosis factor alpha; TLR2, toll like recptor 2, TLR4, toll like receptor 4; IL-1β, interleukin 1 beta; IL-1 interleukin 1; IL-6, interleukin

REFERENCES

AHMED, S. et al. A review on plants extract mediated synthesis of silver nanoparticles for antimicrobial applications: A green expertise. **Journal of Advanced Research**, v. 7, n. 1, p. 17–28, 2016.

AHMED, T. A.; ALJAEID, B. M. Preparation, characterization, and potential application of chitosan, chitosan derivatives, and chitosan metal nanoparticles in pharmaceutical drug delivery. **Drug Design, Development and Therapy**, v. 10, p. 483–507, 2016.

ALETAHA, D. et al. **2010 Rheumatoid arthritis classification criteria: An American College of Rheumatology/European League Against Rheumatism collaborative initiativeArthritis and Rheumatism**, 2010.

ALLEN, T. M.; CULLIS, P. R. **Liposomal drug delivery systems: From concept to clinical applicationsAdvanced Drug Delivery Reviews**, jan. 2013.

ALMEIDA, D. E. DE et al. IMMUNE DYSREGULATION BY THE RHEUMATOID ARTHRITIS SHARED EPITOPE. **Journal of Immunology**, v. 185, n. 3, p. 1927–1934, 2011.

ASHAI, Z. A. et al. Nanopharmacology. **JK-Practitioner**, v. 17, n. 1–3, p. 83–85, 2012.

BADER, R. A. The Development of Targeted Drug Delivery Systems for Rheumatoid Arthritis Treatment. In: LEMMEY, E. BY D. A. (Ed.). . **Rheumatoid Arthritis Treatment**. IntechOpen ed. Bangor. p. 111–124.

BALE, S. et al. Overview on therapeutic applications of microparticulate drug delivery systems. **Critical Reviews in Therapeutic Drug Carrier Systems**, v. 33, n. 4, p. 309–361, 2016.

BERNARDI, A. et al. THEMED SECTION : MEDIATORS AND RECEPTORS IN THE RESOLUTION OF INFLAMMATION Effects of indomethacin-loaded nanocapsules in experimental models of inflammation in rats. **British Journal of Pharmacology**, v. 158, n. 4, p. 1104–1111, 2009.

BERTRAND, N. et al. Cancer nanotechnology: The impact of passive and active targeting in the era of modern cancer biology. **Advanced Drug Delivery Reviews**, v. 66, p. 2-25, 2014.

BOECHAT, A. L. et al. Methotrexate-loaded lipid-core nanocapsules are highly effective in the control of inflammation in synovial cells and a chronic arthritis model. **International Journal of Nanomedicine**, v. 10, n. 1, p. 6603–6614, 2015.

BONIFÁCIO, B. V. et al. Nanotechnology-based drug delivery systems and herbal medicines : a review. **International Journal of Nanomedicine**, v. 9, p. 1–15, 2014.

CAMERON, M. et al. Evidence of Effectiveness of Herbal Medicinal Products in the Treatment of Arthritis Part 2 : Rheumatoid Arthritis. **PHYTOTHERAPY RESEARCH**, v. 1662, n. July, p. 1647–1662, 2009.

CHAN, F. K. L. et al. Celecoxib versus omeprazole and diclofenac in patients with osteoarthritis and rheumatoid arthritis (CONDOR): A randomised trial. **The Lancet**, v. 376, n. 9736, p. 173–179, 2010.

CHUANG, S. et al. Lipid-Based Nanoparticles as a Potential Delivery Approach in the Treatment of Rheumatoid Arthritis. **Nanomaterials**, v. 8, n. 42, p. 1–16, 2018.

DEVI, V.; JAIN, N.; VALLI, K. Importance of novel drug delivery systems in herbal medicines. **Pharmacognosy Reviews**, v. 4, n. 7, p. 27–31, 2010.

DINI, V. S. Q. et al. Ação anti-inflamatória do óleo de copaíba em artrite induzida em modelo animal : Uma Revisão Sistemática. **Scientia Amazonia**, v. 8, n. 1, p. 1–12, 2019.

DUAN, W.; LI, H. Combination of NF-kB targeted siRNA and methotrexate in a hybrid nanocarrier towards the effective treatment in rheumatoid arthritis. **Journal of Nanobiotechnology**, v. 16, n. 1, p. 1–9, 2018.

DUDICS, S. et al. Natural Products for the Treatment of Autoimmune Arthritis : Their Mechanisms of Action , Targeted Delivery , and Interplay with the Host Microbiome. **International Journal of Molecular Sciences**, v. 19, n. 9, p. 2508, 2018.

FAN, Z. et al. Anti-Inflammation and Joint Lubrication Dual Effects of a Novel Hyaluronic Acid/Curcumin Nanomicelle Improve the Efficacy of Rheumatoid Arthritis Therapy. **ACS Applied Materials & Interfaces**, v. 10, p. 23595–23604, 2018.

FERREIRA, J. F.; AHMED MOHAMED, A. A.; EMERY, P. Glucocorticoids and Rheumatoid Arthritis**. Rheumatic Disease Clinics of North America**, v. 42, n. 1, p. 33-46, 2016.

FISSELL, W. H. What Is Nanotechnology?. **Advances in Chronic Kidney Disease**, v. 20, n. 6, p. 452-453, 2013.

FRANK, L. A. et al. Improving drug biological effects by encapsulation into polymeric nanocapsules. **Nanomedicine and Nanobiotechnology**, v. 7, n. 5, p. 623–639, 1 set. 2015.

GESZKE-MORITZ, M.; MORITZ, M. Solid lipid nanoparticles as attractive drug vehicles: Composition, properties and therapeutic strategies. **Materials Science and Engineering C** Elsevier Ltd, v. 68, p. 982-994, 2016.

GU, Y. et al. Transdermal drug delivery of triptolide-loaded nanostructured lipid carriers: Preparation, pharmacokinetic, and evaluation for rheumatoid arthritis. **International Journal of Pharmaceutics**, v. 554, n. September 2018, p. 235–244, 2019.

HELMY, H. S. et al. Therapeutic effects of lornoxicam-loaded nanomicellar formula in experimental models of rheumatoid arthritis. **International Journal of Nanomedicine**, v. 12, p. 7015–7023, 2017.

JANAKIRAMAN, K. et al. Novel nano therapeutic materials for the effective treatment of rheumatoid arthritis-recent insights. **Materials Today Communications**, v. 17, p. 200–213, 1

dez. 2018.

JIN, K. et al. Biomimetic nanoparticles for inflammation targeting. **Acta Pharmaceutica Sinica B**, v. 8, n. 1, p. 23–33, 2018.

JURENKA, J. S. Anti-inflammatory Properties of Curcumin , a Major Constituent of Curcuma longa : A Review of Preclinical and Clinical Research. **Alternative Medicine**, v. 14, n. 2, 2009.

KOTHAMASU, P. et al. Nanocapsules: The weapons for novel drug delivery systems. **BioImpacts**, v. 2, n. 2, p. 71–81, 2012.

KUMAR, R. et al. Solid lipid nanoparticles for the controlled delivery of poorly water soluble non-steroidal anti-inflammatory drugs. **Ultrasonics Sonochemistry**, v. 40, p. 686–696, 1 jan. 2018.

LAMBERT, D. G. Disease-modifying antirheumatic drugs. **Anaesthesia and Intensive Care Medicine**, v. 13, n. 3, p. 128–130, 2012.

LI, Z. et al. Glycyrrhetinic Acid Accelerates the Clearance of Triptolide through P-gp In Vitro. **PHYTOTHERAPY RESEARCH**, v. 1096, n. May, p. 1090–1096, 2017.

MAHMOOD, A.; MAHMOOD, A.; TABASSUM, A. Ethnomedicinal Survy of Plants From District Sialkot, Pakistan. **Journal of Applied Pharmacy**, v. 3, n. 3, p. 212–220, 2018.

MATTA, R. et al. Triptolide induces anti-inflammatory cellular responses. **American Journal of Translational Research**, v. 1, n. 3, p. 267–282, 2009.

MCINNES, I. B.; SCHETT, G. The Pathogenesis of Rheumatoid Arthritis. **The New England Journal of Medicine**, v. 365, p. 2205–2219, 2011.

MELLO, S. B. et al. Intra-articular methotrexate associated to lipid nanoemulsions : anti-inflammatory effect upon antigen-induced arthritis. **International Journal of Nanomedicine**, v. 8, p. 443–449, 2013.

MOGHADAMTOUSI, S. Z. et al. A Review on Antibacterial , Antiviral , and Antifungal Activity of Curcumin. **BioMed Research Internationa**, v. 2014, p. 1–12, 2014.

NGUYEN, C. N. et al. Nanostructured lipid carriers to enhance transdermal delivery and efficacy of diclofenac. **Drug Delivery and Translational Research**, v. 7, n. 5, p. 664–673, 2017.

PRABHU, P. et al. Investigation of nano lipid vesicles of methotrexate for anti-rheumatoid activity. **International Journal of Nanomedicine**, v. 7, p. 177–186, 2012.

ROOME, T. et al. Opuntioside, opuntiol and its metallic nanoparticles attenuate adjuvant-induced arthritis: Novel suppressors of Toll-like receptors -2 and -4. **Biomedicine and Pharmacotherapy**, v. 112, n. August 2018, p. 108624, 2019.

SHAO, P. et al. Modulation of the immune response in rheumatoid arthritis with strategically released rapamycin. **Molecular Medicine Reports**, v. 16, p. 5257–5262, 2017.

SHARMA, J.; BHAR, S.; DEVI, C. S. A review on interleukins: The key manipulators in rheumatoid arthritis. **Modern Rheumatology**, v. 27, n. 5, p. 723–746, 2017.

SHI, Q. et al. In vivo therapeutic efficacy of TNFα silencing by folate-PEG-chitosan-DEAE/siRNA nanoparticles in arthritic mice. **International Journal of Nanomedicine**, v. 13, p. 387–402, 2018.

SIDDIQUI, F. et al. Analgesic potential of Opuntia dillenii and its compounds opuntiol and opuntioside against pain models in mice. **Records of Natural Products**, v. 10, n. 6, p. 721–734, 2016.

SINGH, Y. et al. Nanoemulsion: Concepts, development and applications in drug delivery. **Journal of Controlled Release,** Elsevier B.V., v. 252, p. 28-49, 2017.

SMOLEN, J. S.; ALETAHA, D.; MCINNES, I. B. Rheumatoid arthritis. **The Lancet**, v. 388, n. 10055, p. 2023–2038, 2016.

SONG, Y. W.; KANG, E. H. Autoantibodies in rheumatoid arthritis: Rheumatoid factors and anticitrullinated protein antibodies. **QJM**, v. 103, n. 3, p. 139-146, 2009.

STROHL, W. R. The role of natural products in a modern drug discovery program. **Drug Descovery Today**, v. 5, n. 2, p. 39–41, 2000.

TAYAL, S. **The Role of Lornoxicam in Pain and Inflammation: A Review**. Disponível em: <http://crpsonline.com/index.php/crps/article/view/45/31>. Acesso em: 6 fev. 2020.

VADLAPUDI, A. D.; MITRA, A. K. Nanomicelles: an emerging platform for drug delivery to the eye HHS Public Access. **Therapeutic Delivery**, v. 4, n. 1, p. 1–3, 2013.

WANG, Y. et al. Manufacturing techniques and surface engineering of polymer based nanoparticles for targeted drug delivery to cancer. **Nanomaterials**, v. 6, n. 2, 1 fev. 2016.

YU, C. et al. Hyaluronic Acid Coated Acid-Sensitive Nanoparticles for Targeted Therapy of Adjuvant-Induced Arthritis in Rats. **Molecules**, v. 24, n. 1, p. 146, 2019.

ZHANG, L. et al. Fabrication of a triptolide-loaded and poly-γ-glutamic acid-based amphiphilic nanoparticle for the treatment of rheumatoid arthritis. **International Journal of Nanomedicine**, v. Volume 13, p. 2051–2064, 2018.

ZHAO, J. et al. Multifunctional folate receptor-targeting and pH- responsive nanocarriers loaded with methotrexate for treatment of rheumatoid arthritis. **International Journal of Nanomedicine**, v. 12, p. 6735–6746, 2017.

ZHOU, M. et al. Targeted delivery of hyaluronic acid-coated solid lipid nanoparticles for rheumatoid arthritis therapy. **Drug Delivery**, v. 25, n. 1, p. 716–722, 2018.

CHAPTER 2 - Research Article

The Anti-arthritic Activity of Diclofenac Lipid-Core Nanocapsules: Stereological Analysis Showing Deep Joint Components Protection

1. Introduction

Non-steroidal anti-inflammatory drugs (NSAIDs) are the most prescribed medication to treat the pain and stiffness caused by Rheumatoid Arthritis (THAKUR et al., 2018). NSAIDs act via the inhibition of cyclooxygenase (COX) enzymes, blocking the production of prostanoids (prostaglandins [PGs], prostacyclin [PGI2] and thromboxane [TX]) which promote the swelling of the inflamed tissue (HUNT et al., 2009; KU et al., 1986).

Worldwide, Diclofenac is the most prescribed NSAID and can inhibit both isoforms of cyclooxygenase, COX-1 and COX-2 (ALTMAN et al., 2015). Diclofenac gives temporary relief for the symptoms of RA and is usually an adjunct measure, used in combination with other drugs, like glucocorticoids. Non-steroidal anti-inflammatory drugs do not alter the progression of the RA and long term use generates serious side effects (CROFFORD, 2013). Some of the adverse effects caused by the NSAIDs are esophagitis, peptic ulcer, peptic ulcer complications, bleeding, occult blood loss, development of anemia and death. All of these side effects are caused by the poor selectivity for inflamed tissue (LANAS, 2009; CHAN et al., 2010).

To overcome this difficulty, nanotechnology synthesizes nanopharmaceuticals that travel to targeted areas of inflammation, avoiding the possible side effects that drugs can cause to the system (PRASAD; O'MARY; CUI, 2015). Studies have demonstrated the enhanced anti-inflammatory activity and strong modulation of pro-inflammatory mediators that NSAIDs develop when used in nanostructure vehicles (CHIONG et al., 2013; TURK et al., 2013).

Lipid-core polymeric nanocapsules (LNC) are a type of polymeric nanoparticles constituted by a polymeric wall and an organo-gel core containing a dispersion of sorbitan

monostearate in medium-chain triglycerides, stabilized by polysorbate 80 micelles (JÄGER et al., 2009; VENTURINI et al., 2011; FIEL et al., 2013). Recent studies have demonstrated diclofenac acid is loaded in Lipid-core nanocapsules with high efficiency and is distributed mainly in the pseudo-phase interface of the LNC[4] which can conduce to decrease the dose to elicit the necessary therapeutic activity and the side effects. The use of the LNC has shown many advantages like a decreased TNFα, IL-1 and IL-6 level and increased the IL-10 level in the arthritis model using a LNC loaded indomethacin (BERNARDI et al., 2009)

In the effort to understand Rheumatoid Arthritis, many studies have been using Stereology as a tool to quantify the morphological changes caused by this disease (KELLER et al., 2012; KELLER et al., 2013). Stereology is defined as “The body of methods for the investigation of three-dimensional space when only two-dimensional sections through solid bodies or their projections on a surface are available" (EXNER, 2011).

The application of Stereology provides the calculation of volume, density and the counting of structures of one determinate object, through the analysis of 2 dimension images. Helping obtain accurate results with minimum bias through the evaluation of serial sections made from the object of interest (BOYCE et al., 2010). Studies have proven the efficacy that this technique has on the analysis of experimental models of arthritis (SILVA et al., 2004; THOTE et al., 2013). But even with all of the breakthroughs and advances on the research of Rheumatoid Arthritis, there is still a gap in identifying the onset, progression and cure for this disease.

Previously we had tested a lipid-core nanocapsule loaded with methotrexate (MTX) and observed the many anti-inflammatory and immunomodulation advantages that it provided on an experimental model of arthritis (BOECHAT et al., 2015). We hypothesize that the Diclofenac Lipid-core Nanocapsule (DIC-LNC) preserve the chondrocytes, synovial space and diminish synovitis of the arthritic joints. The aim of this work is to evaluate, through stereological analysis, the anti-arthritic activity of DIC-LNC in an experimental model of arthritis.

2. Materials and Methods

2.1 Materials

Poly(ε-caprolactone) (PCL) (Mw = 65 000g.mol-1) and sorbitan monostearate (Span 60®) were supplied by Sigma-Aldrich Co. Caprylic/capric triglyceride (CCT) was obtained from Delaware (Brazil) and polysorbate 80 was obtained from Brasquim (Brazil). Sodium diclofenac was obtained from Galena (Brazil). All other chemicals and solvents used were of analytical or pharmaceutical grades. All reagents were used as received.

2.2 Preparation of the lipid-core nanocapsules formulations

Firstly, the acid diclofenac was obtained by methodology previously described [6,4] (BECK et al 2004; OLIVEIRA et al 2013;) in which the aqueous medium containing sodium diclofenac was acidified with 5mol.L^{-1} hydrochloric acid until turbidity was observed. So, that mixture was kept static to allow precipitation in a cooling bath and the precipitate obtained was filtered and recrystallized using water: ethanol (1:1 v/v). The colorless crystals were characterized by infrared spectroscopy (FT-IR 8300, Shimadzu) and presented lmax (cm-1) of 3300 (NH), 3200-2500 (OH) and 1710 (C=O).

The Formulations containing or not acid diclofenac denominated DIC-LNC and LNC, respectively, were prepared by interfacial deposition of preformed polymer methodology previously reported 1,4 (VENTURINI et al 2011; OLIVEIRA et al 2013). The organic phases, at 40ºC, composed by acetone solution (27 mL), PCL (0.100 g), sorbitan monostearate (0.038 g), capric/caprylic triglyceride (0.160 g) and containing (DIC-LNC) or not (LNC) acid diclofenac (0,010 g) was poured into the aqueous phases (53 mL) containing polysorbate 80 (0.077 g) at 40ºC and a turbid solution was obtained instantaneously. Afterward, acetone was removed and the suspension was concentrated under reduced pressure at 40ºC. The final volume was adjusted to 10 mL in a volumetric flask.

2.3 Physicochemical characterization of the formulations

pH measurements

After preparation, the pH values of formulations were determined without previous dilution. To this were used a calibrated potentiometer B-474 (Micronal, Brazil) equipped with an Ag electrode/AgCl (Analion V620), at room temperature.

Electrophoretic mobility and zeta potential

The Zeta potential values were measured using the aforementioned Zetasizer® Nano ZS (Malvern Instruments Ltd., UK) based on electrophoretic mobility. The samples were dispersed in 10mM NaCl aqueous solution (500 times diluted) and the analysis was realized at 25 ºC.

Particle sizing

Laser diffraction

The granulometric profile of the DicOH-LNC and LNC formulations were obtained by laser diffraction (Malvern Mastersizer® 2000, Malvern Instruments, UK), with added directly in the instrument containing distilled water, at room temperature. Formulations were analyzed using an obscuration between 2 and 8 % and were determined the median diameter based on the volume-weighted mean diameters (D[4.3]) and the polydispersity of particle sizes (Span, based on 10%, 50% and 90% of the cumulative size distribution).

Dynamic Light Scattering

Formulations were analyzed by dynamic light scattering (DLS) using ZetaSizer Nano ZS (Malvern Instruments Ltd., UK) to determine the hydrodynamic diameter (Dh), using the method of Cumulants, and the polydispersity index, using the relative variance in the particle size distribution, of the lipid-core nanocapsules in the range from 1 nm to 5 μm, formulations were diluted 500 times in ultrapure water (MilliQ®) and analyzed an angle of 173 °, at 25 °C.

Nanoparticle tracking analysis

Nanoparticle Tracking Analysis (NTA) was realized using a NanoSight instrument (LM10, NanoSight Ltd., Amesbury, UK) after the formulations were diluted (5000 x) in pre-filtered water (MilliQ®). By Brownian motion of the lipid-core nanocapsules, the hydrodynamic diameter (Dh) the median diameter (D50), the diameter at the 90th percentile (D90) under the cumulative size distribution and the particle number density (PND) were obtained in real-time via a CCD camera. The video clips were captured over 60 s, at 21.6±0.5 °C and 0.96 ± 0.02 cP.

Drug content and Encapsulation Efficiency

The drug content of the acid diclofenac in DicOH-LNC were quantified by high-performance liquid chromatography (HPLC, Perkin Elmer S-200 with an S-200 injector) using a UV-VIS detector, 280 nm and mobile phase consisted of acetonitrile: water (65:35 v/v) adjusted to an apparent pH of 5.0±0.5 with 10% (v/v) acetic acid, with a flow rate of 1.0mL min-1 and injection volume of the 20 µL7. The sample was diluted in acetonitrile in a volumetric flask and filtered with 0.45 µm membranes (Millipore, USA). The methodology presented proper linear regression, with r>0.999 in the interval used, 1-50 µg.mL-1, and demonstrated specificity, accuracy (99±1 %), repeatability and precision (relative standard deviation <5%).

The encapsulation efficiency (EE) was established by ultrafiltration-centrifugation by added of the 300 µL of the formulation, without previous dilution, in a Microcon® centrifugal filter device (10KDa, Millipore®, USA), after this was centrifuged at 1844 x g (RCF) for 5 min using a centrifuge (Sigma® 1-14, Germany) and the ultrafiltrate was analyzed by HPLC with the method above described. The EE was calculated from the difference between the total drug content (total concentration of the drug in the formulation) and the drug concentration in the ultrafiltrate (concentration of dissolved drug in the continuous phase). All analyses were made in triplicate.

2.4 Animals

Twenty 8-week-old Lewis rats that weighed between 250 and 350 g were maintained in the biotherium at the Federal University of Amazonas (UFAM) and used in the experiment. The animals had access to water and food and were maintained in a light-controlled (12-

hour light-dark cycle) and temperature-controlled (22°C) environment. They were allocated by simple randomization into four groups, four animals were maintained in each cage and one animal was kept alone for negative control. All experiments were performed with the approval of the Institutional Committee for Ethics in Animal Experiments under reference number 010/2010 (CEEA) UFAM.

2.5 Induction of arthritis by Freund's Complete Adjuvant and Experimental Design

The induction of arthritis was made through an intradermal injection on the tail of the rats with 0.1 mL of complete Freund's adjuvant (Difco) after the inhalation of anesthesia with isoflurane, on the first day of the experiment. After the evidence of arthritis, the animals were allocated into four groups using simple randomization: Group 1: control (arthritic rats without treatment), Group 2: arthritis with empty LNC, Group 3: arthritis with a free solution of Diclofenac and Group 4: arthritis with the nanoformulation DIC-LNC. On the 14th day of the experiment, each treatment was initiated with an intraperitoneal injection of DIC, DIC-LNC and empty LNC, respectively for each group. The DIC dissolved in saline solution creating a final dose of 1mg/mL. The DIC dose was 3 mg/kg/day. On day 28 of the experiment, the animals were killed by inhalation of isoflurane and blood was obtained by heart puncture.

2.6 Randomization, Blinding and Allocation Concealment

To allocate animals into a treatment group, a list of random numbers was used and the animals were raffled by simple randomization (randomization.com.br). Allocation concealment was achieved by a codified random list produced by personnel that was not involved with experiment design nor conducting. All animal treatment assessments, biochemical markers, stereological and data analysis were conducted under blinding evaluation.

2.7 Edema volume and arthritis score of the hind paw

The volumes of the paws were measured on days 0, 7, 14, 21 and 28 of the experiments, with a digital plethysmometer (Insight®, Brazil). The paws volume measurements were assessed by a blind evaluator. The arthritis score was evaluated on the 28th day of the

experiment. The categorization was assessed observing the signs of erythema, swelling and deformity of the paw, designated as follows: score 0- no erythema or swelling-, score 1 – minimal erythema or swelling of a toe or finger; score 2 – erythema and swelling of more than one toe or finger; score 3 – erythema and swelling of more than one toe of finger with inclusion of ankle or wrist; and score 4 – complete erythema and swelling of the paw, including toes or fingers and the ankle or wrist and loss of ability to bend the ankle or wrist. The four paws of the rats were scored; the highest possible arthritic index score was 16.

2.8 Quantification of cytokines and biochemical markers

With a CBA Flex Sets® (cytometry bead array) the serum levels of TNF-α, IL-1α and CRP were measured, following the manufacturer's instructions. To read the samples a FACSCalibur™ flow cytometer (BD Biosciences) was used. The quantity and mean fluorescence of the cytokines were calculated using BD FCAP Array™ Software (v 1.0.1; BD Biosciences). To calculate the serum levels of CRP, a Roche Hitachi Chemistry Analyzer and immunoturbidimetric assay (catalog number: 4956842190) was used following the manufacturer's instructions. Liver and renal toxicity were evaluated measuring glutamic oxaloacetic transaminase (TGO), glutamic pyruvic transaminase (TGP), gama glutamyl transpeptidase (GGT) and alkaline phosphatase (FAL), creatinine and blood urea nitrogen (BUN).

2.9 Stereological analysis

After the euthanasia, the left and right hind paws were removed and preserved in buffered formaldehyde 10% until the stereological analysis. Each paw was previously codified according to group allocation and all stereological analyses were performed under allocation concealment strategy. The rat paws were washed in distilled water to remove any residue of formaldehyde. Then, the second digit of the paws were removed, since the articulation of interest was the metatarsophalangeal (MTP) of the second digit. The hair and skin of the digits were peeled for better absorption of the decalcifier substance. All the digits were kept in 10% Formic Acid for 48hrs until complete decalcification.

After this, they were washed in distilled water and dehydrated in an alcoholic series (70% and 96%), following resin embedding (Technovit 7100, Külzer-Heraues, Germany). Each block containing the finger was kept in a stove at 50o C for 24 hrs.

After this, each block was positioned in an angle clock and randomly rotated to create different angles for sectioning, according to the principle of vertical sectioning (BADDELEY; GUNDERSEN; CRUZ-ORIVE, 1986). Figure 1 shows the procedure used to obtain the vertical sections of the MTP joint. Ten to eleven sections **(**5 □m thick) were taken with a constant distance (*T*) of 50 □m for each block using a microtome (Leica RM 2145, Germany). The sections were stained with toluidine blue 0.5% (toluidine blue, 0.12 g; Na^+ borate, 0.5 g; distilled H_2O, 100 mL) and basic fuchsine (basic fuchsine, 0.5 g and distilled H_2O, 100 mL). All these procedures for histological evaluation were described by Kiernan (1999).

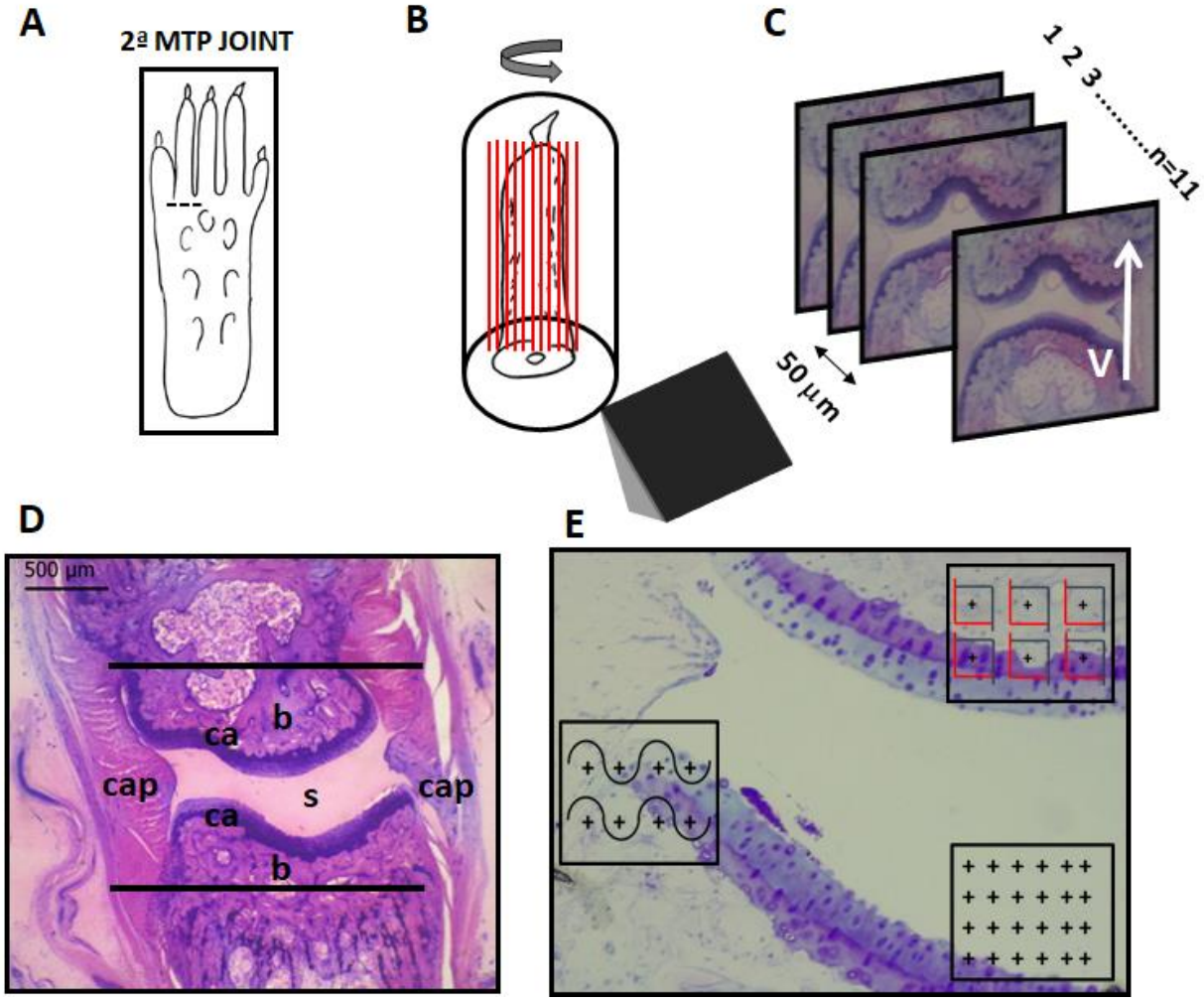

Figure 1. Methods used for stereological analysis. A. Sectioning level of the 2nd digit of the paw. **B**. Block of resin containing an MTP joint (longitudinal lines indicate the location of the knife during the cuts with the microtome). **C.** Generation of 50µm equidistant serial sections. Any section passing through the longitudinal plane of the finger will be a vertical section. **D**. Profile of a section used to determine Cavalieri volume. In this magnification (8) the structures marked in the image are fully visible. The lines delimit the area investigated in this study limited by the border with the spongy bone **E**. Detail of the articular region used to estimate the volume density (point-counting system), surface area (counting system with points and curves) and number of chondrocyte profiles (counting system with frames and a central point). cap, capsule; b, bone; ca, cartilage; s, synovial space.

2.10 Determination of Cavalieri's Volume

The volume of MTP joint was determined according to Cavalieri's principle (LOCKWOOD; EVES, 2007; GUNDERSEN; JENSEN, 1987). This principle is used when the precise

calculation of any volume is needed. For this matter, all the serial sections of each block were digitized by the stereomicroscope (Leica EZ4D Digital System, Germany) and through the program of *Imod* 4.7/ *stereology* (KREMER; MASTRONARDE; MCINTOSH, 1996) a counting system of points was overlap on each section. The procedure consists of counting all the points hitting the MTP joint (defined by the limits of the capsule). The volume was estimated using the following formula:

$$\boldsymbol{V}\ (\boldsymbol{mm^3}) = \sum_{\boldsymbol{i=1}}^{\boldsymbol{m}} \boldsymbol{Pi}\ \times \boldsymbol{T}\ \times \boldsymbol{a/p}$$

Where, V was the absolute volume of the MTP joint; ∑Pi was the sum of points hitting MTP; a/p was the area occupied by each central point (23470 μm^2) and T (50 μm) was the distance between each section (GUNDERSEN; JENSEN, 1987).

2.11 Determination of Relative Volume

The percentage of each component within MTP was obtained by the Delesse principle (DELL'ISOLA; GUARASCIO; HUTTER, 2000). For this, microscopic fields of view within the joint were systematic, uniform and random sampled (magnification 200). Following the same procedure, a point counting system was superimposed over the images. The percentage of the volume occupied by each component in relation to the reference space (joint) was calculated as:

$$\boldsymbol{Vv}\ (\boldsymbol{component, reference\ space}) = \frac{\sum_{\boldsymbol{i=1}}^{\boldsymbol{m}} \boldsymbol{Pcomp}}{\sum_{\boldsymbol{i=1}}^{\boldsymbol{m}} \boldsymbol{Pref}}$$

Where *Vv* was the volume density of articular component; ∑Pcomp was the sum of points hitting each component (capsule, synovial space, and synovial membrane) and ∑Pref was the sum of points hitting the reference space (articular region) (HOWARD; REED, 1998). The percentage values obtained for each component were transformed into absolutes when multiplied by Cavalieri's volume of the joint, as seen on the next formula:

$$\boldsymbol{Absolut\ Volume}(\boldsymbol{mm^3}) = \boldsymbol{Vv\ x\ Cavalieri\ Volume}$$

2.12 Determination of Surface Area

The same images from the preview calculation of Delesse Volume, were used to obtain the surface area of the articular cartilage and synovial membrane. Once again a counting system with long cycloids curves and points was superimposed over the images. Each time a curve intercepted the edge of the cartilage in contact with the synovial space or the synovial membrane, it was counted. The same thing happened with the points that touched these structures. The density of the surface was calculated as:

$$\boldsymbol{Sv\ (mm^{-1}) = \frac{2\sum_{i=1}^{m} I}{\sum_{i=1}^{m} Pi\ \times \frac{l}{p}}}$$

Where *Sv* stands for surface density, *∑I* is the sum of intersections, *∑P* is the sum of points and *"l/p"* is the length of the test curve per grid point. The relative values obtained for each component were transformed into absolutes when multiplied by Cavalieri volume of the joint, see next formula:

$$\boldsymbol{Surface\ area\ (mm^{-1}) = Sv\ x\ Cavalieri\ Volume}$$

2.13 Counting number of cellular profiles

To determine the number of chondrocyte profiles, present in articular cartilage, we used a 2-D quantification technique. The counting system consists of six frames (2700,28 μm^2) and each frame contains a reference point. The counting frames consisted of a solid forbidden line and a dashed acceptance line. Only the nucleus of the cells that appear inside the counting frame and did not touch the exclusive line, were counted. The number of cells was expressed as profiles/mm^2 and calculated with the following formula:

$$\boldsymbol{Nv = \frac{\sum_{i=1}^{m} Q -}{Nf\ X\ Af}}$$

Where: ∑Qchon was the profile cellular number of chondrocytes; and ∑Nframes was the sum of all the analyzed molding frames; and Aframe was the area of the molding frame.

2.14 Statistical Analysis

Data were expressed as means and standard deviations. The results are expressed as the means and standard deviations, and a 95% confidence interval was used. One-way or Two-way ANOVA were used to compare the means, and a Tukey's test or linear test for trend was used for post hoc analysis. The Mann-Whitney test was used when normality was not observed by the Barllet analysis. Linear regression and curve-fitting with non-linear polynomial regression were applied to study the effects of the different MTX preparations on cytokine levels in the blood and synovial culture cells. A significance level of α=0.05 was adopted, and all p-values were two-tailed. The level of significance used was 5%. For stereology analysis, the variance was expressed as the coefficient of error (*CE*) for each parameter evaluated (V, Vv and Sv). The accuracy of the Cavalieri volume estimate was determined according to (CRUZ-ORIVE 1999),

$$\mathbf{CE} = \left[\mathbf{0,0724} \times \frac{\boldsymbol{B}}{\sqrt{\boldsymbol{A}}} \times \frac{\sqrt{\boldsymbol{n}}}{\left(\sum_{\boldsymbol{i=1}}^{\boldsymbol{m}} \boldsymbol{Pi}\right)^{\frac{3}{2}}} \right]^{\frac{1}{2}}$$

Where *CE* indicates the coefficient of error for Cavalieri's volume determination; $\frac{\boldsymbol{B}}{\sqrt{\boldsymbol{A}}}$ indicates the variance in the count on the sections (shape coefficient) and depends on the morphological complexity of the structure; *n* represents the number of sections evaluated and is the number of points counted on the sections.

3. Results

3.1 Preparation of DIC-LNC dispersed in water

Lipid-core nanocapsules loaded acid diclofenac, DIC-LNC, and lipid-core nanocapsules, LNC, presented white-bluish opalescent liquids with Tyndall effect (visual aspect). The granulometric profile of the DIC-LNC and LNC (**Figure 2**) obtained by Laser diffraction (LD) analysis indicated a monomodal distribution with D[4.3] below 204±46 nm (Span < 1.7) to both formulations. No micrometer particle populations were formed whatever the

formulations, contained or not acid diclofenac. Table 3 summarizes all values obtained by different techniques for DIC-LNC and LNC. These formulations also were analyzed by dynamic light scattering (DLS) to improve accuracy in the nanoscale range measurements and showed hydrodynamic diameter (Dh) below 170 nm (PDI<0.1). Besides the DLS, the hydrodynamic diameters of the formulations also were obtained by nanoparticle tracking analysis (NTA). The NTA technique determines the diameters from individual particles by tracking and sizing them by recording the positional changes due to their Brownian movement, the formulations showed Dh between 182 and 196, D90 below the 309 nm and particle number density between 4.76 x 1012 and 4.98 x 1012 particle.mL-1 (**Table 1**).

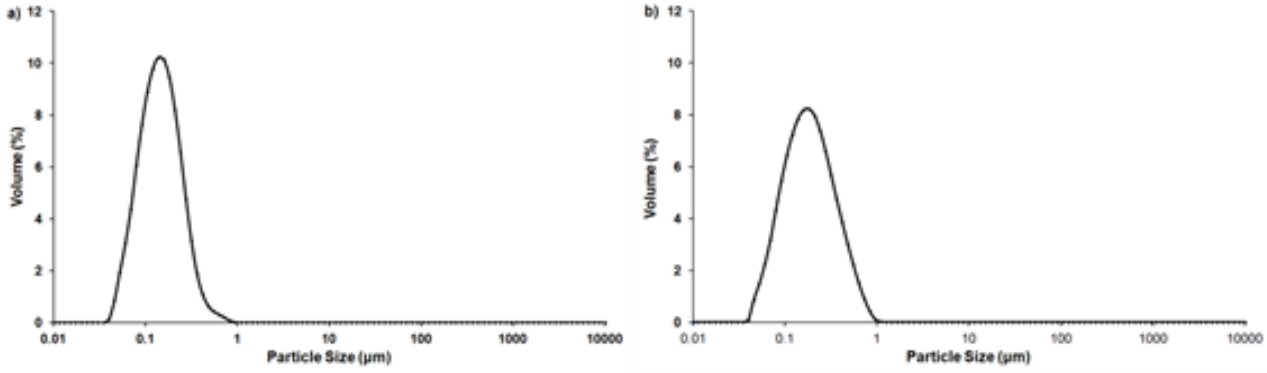

Figure 2. **Granulometric profiles obtained by LD**. a) LNC; b) DIC-LNC. The “X” axis represents Particle size in nm and the “Y” axis represents volume percentage.

Table 1. Characterization of the formulations by potentiometry, laser diffraction, dynamic light scattering and nanoparticle tracking analysis.

	LNC	**DicOH-LNC**
Potentiometry		
pH	5.43±0.24	5.39±0.16
Laser diffraction		

D[4.3] (nm)	153±10	204±46
Span	1.4±0.2	1.7±0.1
Dynamic Light Scattering		
D*h* (nm)	170±13	166±13
PDI	0.06±0.02	0.08±0.02
Electrophoretic mobility Zeta Potential (mV)	-13±6	-11±2
Nanoparticle tracking analysis		
D*h* (nm)	182±9	196±14
D50 (nm)	173±13	186±2
D90 (nm)	257±10	309±9
PND (x10^{12} particles mL^{-1})	4.98±0.25	4.76±0.78

Note: Data are expressed as mean ± standard deviation. **Abbreviations:** LNC, blank lipid-core nanocapsules; DicOH-LNC, acid diclofenac loaded lipid-core nanocapsules; D[4.3], volume-weighted diameter average; D*h*, hydrodynamic diameter; PDI, polydispersity index; D50, median diameter; D90, the diameter at the 90th percentile; PND, particle number density

After assessing the size distribution, the drug loading and encapsulation efficiency of the DIC-LNC were evaluated and the formulation presented drug content of the 1.09±0.10 mg.mL-1 and 100% of the encapsulation efficiency. The pH and the Zeta potential also were evaluated and no significant difference between DIC-LNC and LNC were founded.

3.2 DIC-LNC reduces edema formation at the hind paws

Figure 3 shows edema formation (Panel 2A and 2B) and treatments effect over hind paw volume and arthritis score (Panel C). DIC-LNC reduces paw volume and arthritis score compared to control ($p<0.05$) and DIC ($p<0.05$). Moreover, the treatment effect of DIC-LNC appears to be early on arthritis reduction at 21st day compared to DIC ($p<0.05$).

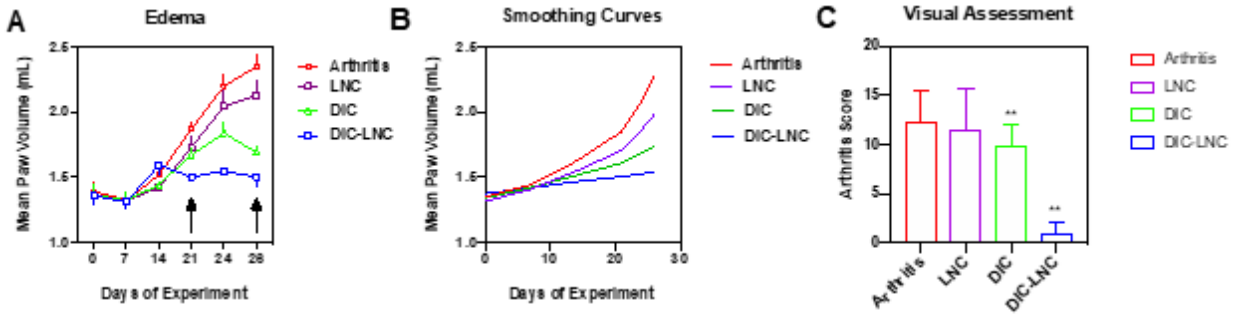

Figure 3 Arthritis evaluation and Scores for twenty-eighty days. **A**. Arthritis kinetics, the black arrows indicate the maximum effects observed; **B** – Edema curve with smoothing techniques and **C** – Arthritis score. ** ($p<0.05$)

3.3 DIC-LNC reduces the serum levels of proinflammatory cytokines and CRP

The serum levels of TNF-α were significantly lower in the DIC-LNC group compared with the DIC group using Tukey's test (p = 0.0114, **Figure 4A**). The serum IL1α levels were similar for both groups when the comparison was performed using a Tukey's test (p = 0.778); however, the linear test for trend indicated a significant trend (p = 0.0001). The CRP levels were also lower for the DIC-LNC group compared with DIC (Mann-Whitney test, p = 0.0286, **Figure 4B**).

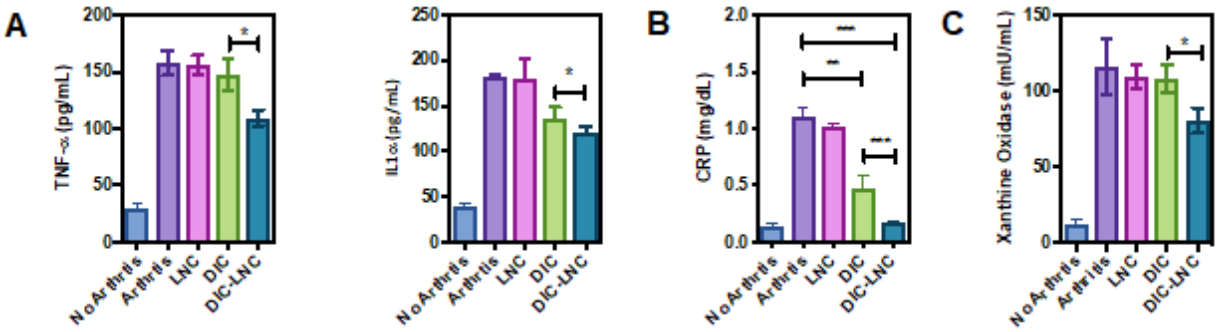

Figure 4. Serum Inflammatory Markers on day twenty-eight of the experiment. **A** – Quantification of the proinflammatory cytokines TNF-α and IL-1α. **B** – Serum levels of CRP for the DIC and DIC-LNC groups and **C –** xanthine-oxidase as an oxidative stress marker**.**

3.4 Absence of liver and renal toxicity with DIC-LNC

To evaluate the liver and kidney toxicity liver enzymes and renal function markers were evaluated **(Figure 5, Panel A and B)**. It was observed that the use of the DIC-LNC did not alter the serum levels of these enzymes (p>0.05) at the doses used at this research,

suggesting no liver toxicity **(Figure 5, Panel A)**. Following the same protocol, the serum levels of creatinine and blood urea nitrogen (BUN) were measured to evaluate renal toxicity **(Figure 5, Panel B)**. It was also observed that the use of the DIC-LNC did not alter the serum levels of BUN nor creatinine, in comparison with the other treatments (p>0.05).

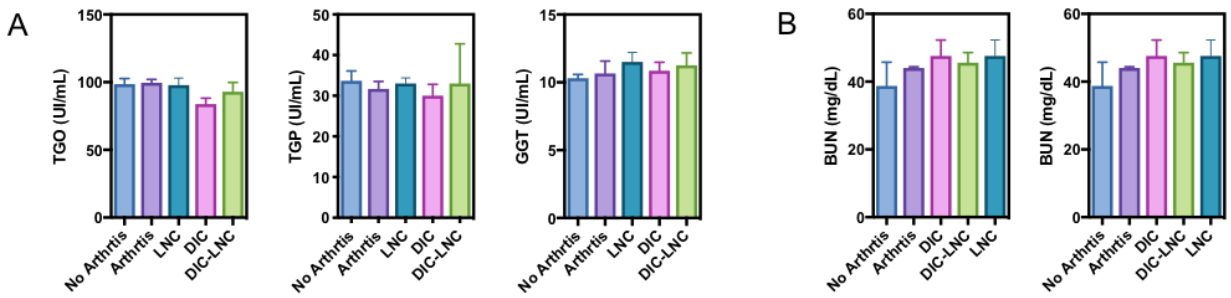

Figure 5. Liver and Kidney Toxicity biochemical markers. A) Liver biochemical markers (TGO, TGP, GGT) of all five groups (Ul/mL). B) Kidney biochemical markers (BUN, CRE) for all five groups (mg/dL).

3.5 Cavalieri's Volume of MTP joints

Figure 6 shows the influence of the number of sections on the efficiency and accuracy of determining the Cavalieri volume of the MTP joint. In a pilot study, a rat's paw finger was histologically processed into resin and thoroughly sectioned to produce 28 sections that were evaluated for the determination of volume according to Cavalieri. A reductive process was applied to show the relationship between the smallest number of sections associated with a low CE. Our results indicated that the use of 10 sections is as accurate as the use of 28 sections and, in addition, it is much more efficient.

Table 2 and Figure 7**(Panel A)** present the results of MTP joint volume. The volume was higher on the Arthritis group when compared with the Diclofenac (p = 0.007) and DIC-LNC group (p < 0.001). Also, the DIC-LNC presented differences with the Diclofenac group (p = 0.023) and the No Arthritis group presented the lowest MTP volume. These results demonstrate that DIC-LNC had an effective diminution of joint volume with values similar to the No Arthritis group.

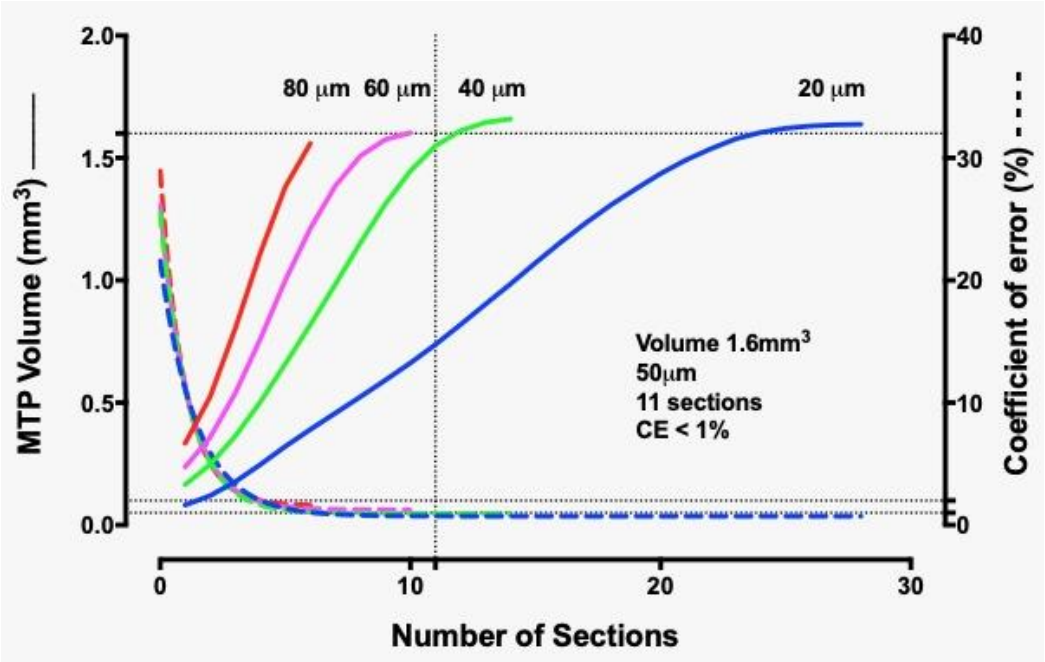

Figure 6. **Relationship between Cavalieri's volume and the coefficient of error**. Demonstration of the relation between the number of serial sections (*x* axis), the volume of Cavalieri (right *y* axis) and the coefficient of error (left *y* axis). Continuous lines indicate the volume and dotted lines represent the respective error coefficient. Blue indicates 28 serial sections equidistant 20 mm; Green indicates 14 40 mm equidistant serial sections; Purple indicates 10 equidistant 60 mm serial sections and red indicates 16 equidistant 80 mm serial sections.

Table 2. MTP Joint volume and Density of its different components

	Volume (mm^3)					
Groups	**Joint**	**Cartilage**	**Bone**	**Capsule**	**Synovial Space**	**Synovial Membrane**
Arthritis	3.02±0.08[1]	0.50±0.10	1.20±0.05	0.97±0.14	0.16±0.01	0.06±0.04
LNC	2.80±0.32[1]	0.36±0.08	1.08±0.16	0.89±0.15	0.17±0.01	0.04±0.01
Diclofenac	2.46±0.12[2]	0.34±0.03	1.02±0.12	0.67±0.02	0.19±0.02	0.03±0.00
Diclofenac-LNC	2.10±0.10[3]	0.21±0.01	0.75±0.05	0.58±0.02	0.26±0.01	0.02±0.00
No Arthritis	1.95±0.05[4]	0.23±0.03	0.61±0.06	0.52±0.03	0.41±0.03	0.01±0.05

Note: Data are expressed as mean ± standard deviation. ANOVA and Turkey's multiple comparisons ($p < 0.001$). **Abbreviations:** LNC, blank lipid-core nanocapsules.

3.6 Density of the joints components and Absolute volume

Table 2 and Figure 7**(Panel B)** summarize the results obtained from the calculation of the relative volume of each component of MTP. The Arthritis group presented an elevated volume of cartilage ($p = 0.0058$; $p < 0.001$), bone ($p = 0.142$; $p < 0.0032$), capsule ($p = 0.142$; $p < 0.0032$) and synovial membrane ($p = 0.003$; $p < 0.001$), when compared with Diclofenac and DIC-LNC groups respectively.

The treatment with DIC-LNC preserved the synovial space ($p = 0.007$) and diminished the volume of cartilage ($p = 0.031$), bone ($p = 0.016$) and synovial membrane ($p = 0.457$) when compared with the Diclofenac group **(Figure 7B)**. Demonstrating that DIC-LNC can cause a diminution of joint inflammation.

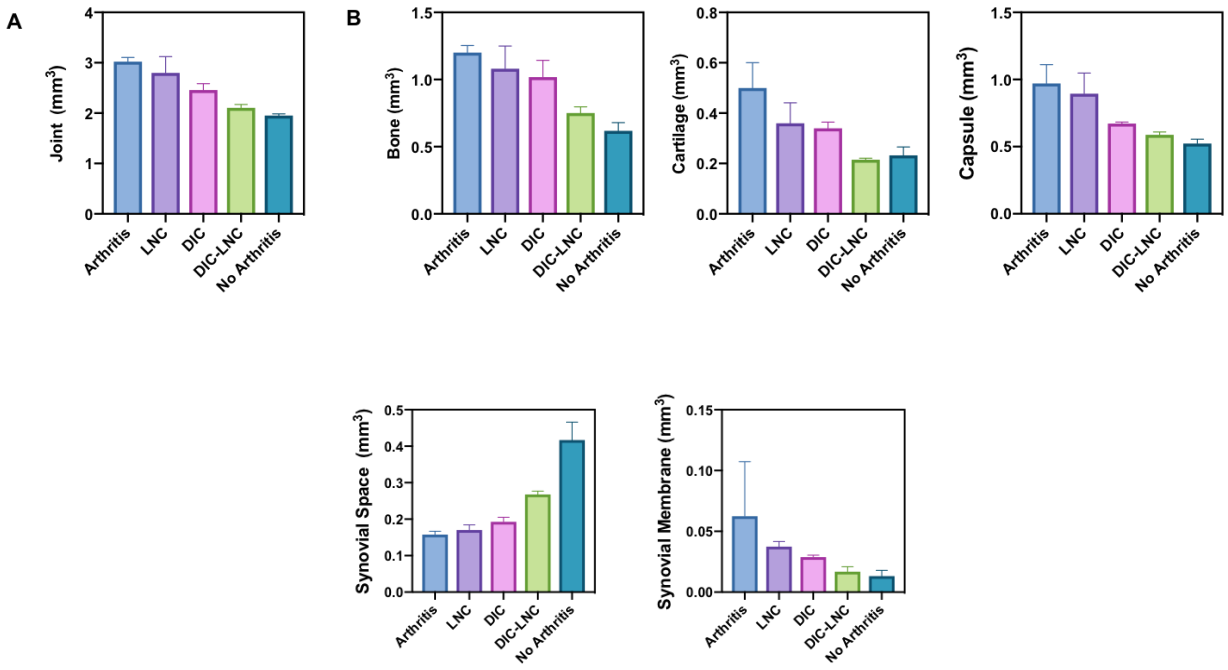

Figure 7. Volume of the MTP joint and density of each component. A) MTP joint volume of all treated groups. B) Absolute volume of the components (Bone, cartilage, capsule, synovial space and synovial membrane) of MTP of each treated group.

3.7 Surface area of MTP joint

Table 3 and Figure 8 **(Panel A)** show the results of surface area of the cartilage and synovial membrane of MTP. The Arthritis group presented the highest surface area of cartilage (p = 0.0011; p = 0.0001) and synovial membrane (p = 0.0058; p = 0.0002) when compared with the Diclofenac and DIC-LNC groups, respectively. As shown in Figure 8, the treatment with DIC-LNC restored the values of cartilage (p = 0.0148) and synovial membrane (p = 0.04) in comparison with Diclofenac group.

Table 3. Surface area and Cellular count of MTP

	Surface Área (mm^2)		Cellular Count ($cell/mm^2$)		
Groups	**Cartilage**	**Synovial Membrane**	**Chondrocytes**	**Isogenous Groups**	**Total chondrocytes**
Arthritis	38.25±4.32	14.22±2.43	1416±126.3	80.55±8.77[1]	1517±54.30
LNC	29.09±3.75	10.42±1.92	1543±49.92	111.5±4.51[2]	1701±91.96
Diclofenac	27.87±3.31	10.06±0.53	1627±95.61	161.1±11.84[3]	1849±16.73
Diclofenac-LNC	20.45±1.58	8.19±0.22	1894±47.00	226.8±20.5[4]	2095±52.33
No Arthritis	19.45±1.28	6.71±1.40	2208±217.4	297.9±19.5[5]	2367±225.8

Note: Data are expressed as mean ± standard deviation.

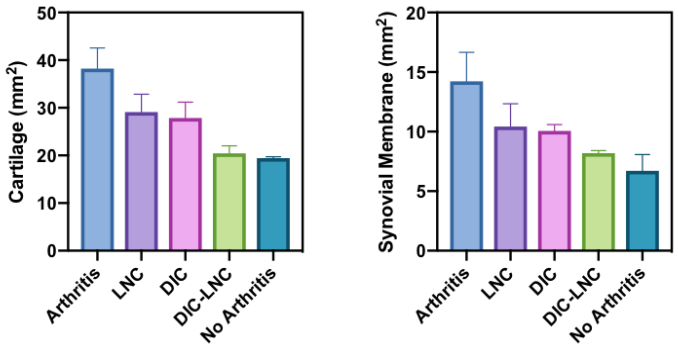

Figure 8. Surface area of MTP. The left panel presents the surface area of the cartilage. The right panel presents the surface area of the synovial membrane.

3.8 Quantification of chondrocytes

Table 3 and Figure 9 summarize the results of chondrocyte count. The No Arthritis group presented the highest number of total chondrocytes. On the other hand, the Arthritis group presented the lowest count of chondrocytes ($p = 0.084$, $p = 0.002$) when compared with Diclofenac and DIC-LNC groups. The Arthritis group also presented a reduction on the number of isogenous groups ($p < 0.001$; $p < 0.001$) and the total number of chondrocytes ($p = 0.004$; $p < 0.001$) when compared with Diclofenac and DIC-LNC groups. The DIC-LNC group presented higher numbers of isogenous groups ($p < 0.001$) and total chondrocytes ($p = 0.004$) when compared with Diclofenac group

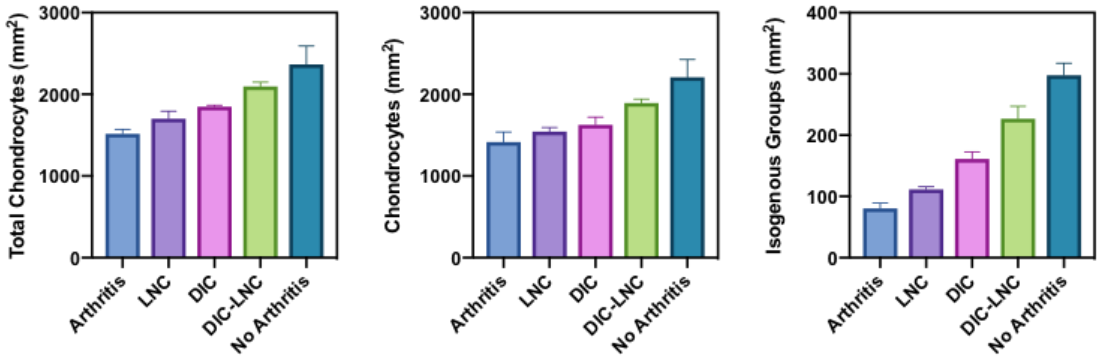

Figure 9. Cellular profile count of MTP chondrocytes. The left panel shows the total number of chondrocytes count. The middle panel shows the number of isolated chondrocytes. The right panel shows the number of isogenous groups of chondrocytes, present after mitosis.

4. Discussion

In this project, we aimed to evaluate through stereological analysis, the activity of DIC-LNC in an experimental model of arthritis. To this end, a lipid core nanocapsule, containing sodium diclofenac, was formulated through the process of interfacial deposition. We demonstrated at this work that, these new diclofenac-loaded lipid-core nanocapsules (DIC-LNC), are able to reduce paw inflammation and cytokine production, preventing synovitis, synovial space and cartilage losses by morphologic quantitative methods. Together, these effects strongly support an anti-arthritic effect for DIC-LNC.

For both formulations, DIC-LNC and LNC, the polydispersity index values were lower than 0.1 indicating a narrow size distribution of the nanoparticles and showed a unimodal

granulometric profile by laser diffraction. Moreover, DIC-LNC presented the size of 204±46nm, a pH of 5.39±0.16 and D*h* above 196 nm and D90 above 309 nm obtained by NTA. These physicochemical parameters show that the nanocapsule is suitable for venous circulation. Lipid-core nanocapsules (LNC) have demonstrated to be effective formulations to entrapped pharmaceuticals (FROZZA et al., 2010) and the deliver drugs in specific areas of inflammation like multiform glioblastoma (BERNARDI et al., 2009), neuroinflammation (BERNARDI et al., 2010) and chronic inflammation (CRUZ et al., 2006). Furthermore, LNCs have been proven to be non-toxic to animal experimental models (BULCÃO et al., 2014). Thus, these nanomaterials are efficient delivering pharmaceuticals to specific areas while minimizing the side effects of the drugs.

Although the success of DMARDS use for rheumatoid arthritis treatment under a treat-to-target approach, pain and inflammation are still challenges at clinical practice (ZANG & LEE, 2018). Proinflammatory cytokines like tumor necrosis factor-alpha (TNF-α), interleukin-1-beta (IL-1β), interleukin-6 (IL-6) and interleukin-17 (IL-17) can rise the peripheral nociceptive neurons sensitization (SCHAIBLE 2014). These cytokines are locally produced by proliferated synovial cells, like macrophages and fibroblasts, and activated T lymphocytes cells at joint inflamed synovia (FIRESTEIN; MCINNES 2017). When proliferated by inflammatory signals, the synovial membrane cells infiltrate joint components and allow cartilage destruction, bone erosion, and joint space narrowing (MCINNES et al 2017). Eicosanoids production at inflamed synovia are both related to pain sensitization and joint inflammation (CROFFORD et al 1994), and are stimulated by inflammatory cytokines (ANDERSON et al 1996; MARTEL-PELLETIER et al 2004).

It has been well known that pro-inflammatory cytokines especially enhance the expression of cyclooxygenase-2 (COX-2) and metalloproteinases (MMP) in human synovial fibroblasts (RASF) (GITTER et al 1989; CROFFORD et al. 1994). Cyclooxygenase and leukotriene inhibition reduce cartilage erosion and bone erosion for both adjuvant arthritis and collagen-induced arthritis (GILROY et al 1989; ANDERSON et al 1996; 2009) Moreover, recent investigations showed that RA patients with optimized treatment highly express cyclooxygenase at the synovial membrane (KOROTKOVA; JAKOBSSON, 2014). When the human cyclooxygenase-2 gene is silenced on cultured synovial cells of

rheumatoid arthritis patients, there is a reduction of prostaglandin E2 (PGE2), vascular endothelial growth factor (VEGF), IL-1β and TNF-α (LENG et al 2018). Taking together, these data may account for those anti-arthritic effects demonstrated for DIC-LNC over conventional diclofenac in experimental arthritis in our work.

With the use of Stereological analysis, it has been proven that there is an augmentation of bone formation in arthritic experimental models. A group of researchers analyzed the bone surface of the joints of arthritic mice. They observed that the mineralizing surfaces of the bone were higher on arthritic mice ($p < 0.001$) when compared with the control group (KRARUP KELLER et al., 2012). This may be explained by the production of TNF-α that promotes the differentiation of osteoclasts in the arthritic joints, which leads to invasion of inflammatory tissue, imbalance of bone resorption/formation and later remodeling of the bone (DIARRA et al., 2007).

In our study, we observed a higher volume of the bone in arthritic joints when compared with the other groups. Also, the experimental model of arthritis used in the project, Adjuvant-Induced Arthritis (AIA), is an aggressive representation of RA that leads to ankyloses and joint malformation. AIA is characterized by inflammation of soft tissue, marked bone loss and periosteal new bone formation (CAI et al., 2006). This data may indicate that the arthritic joints were in the process of joint remodeling.

One marked manifestation of Rheumatoid Arthritis is inflammation of the synovial membrane (SMOLEN; ALETAHA; MCINNES, 2016). In the synovial lining, there is an increase in the activity of fibroblast-like synoviocytes, which produce prostaglandins (PGs) and metalloproteinases (MMPs) that contribute to the destruction of the joint (SMOLEN et al., 2007). Synovitis has been related to the production of TNF-α, IL-17, IL-6, and IL-1. This group of proinflammatory cytokines cause hyperplasia of the synovia and angiogenesis by the activation of macrophages, dendritic cells, T and B lymphocytes (CHOY, 2012).

Synovial membrane augmentation of RA patients was studied using stereological analysis. Researchers observed a significant increase of the synovia when compared with the control group (ARTACHO-PÉRULA et al., 1994). Also applying stereological analysis,

Kristensen et. al, studied the synovial proliferation of arthritic rabbits. The team observed that the arthritic joints of rabbits presented the highest scores of synovial proliferation and thickness when compared with the control group (KRISTENSEN et al., 2008). Our results also show an increase in the volume of the synovial membrane of arthritic joints when compared with the other groups. Making these results coherent with the literature.

Drug nanoencapsulation may increase drug-tissue interactions raising the drug tissue concentration or modified drug biodistribution (FRANK et al 2015). For instance, the ketoprofen-loaded polymeric nanocapsules are able to cross the blood-brain barrier by a passive transport after *in vivo* treatment of glioblastoma in rats (SILVEIRA et al 2013). When nanocapsules are given orally, the adhesion on mucosae improves the performance of the drug nanosystems. Thus, the interaction of indometacin ethyl-ester lipid-core nanocapsules with the gastrointestinal tract acting as a mucoadhesive drug reservoir (CATTANI et al 2010). Of note, nanocapsules are internalized together with the encapsulated substance into the endosomal compartment or in the micronucleus. After that, the drug is then released by simple diffusion, by polymer enzymatic degradation, or by redox-responsive degradation of the polymer.

Recently network metanalysis showed that diclofenac is more likely to control pain, improving physical function with similar adverse effects to other compared NSAID (van WALSEM et al 2015). The diclofenac therapeutic effect for arthritis is largely related to its synovial fluid concentration (FOWLER et al 1983). The synovial bioavailability of diclofenac, on its turn, may be limited by oral absorption and first-pass hepatic metabolism (FOWLER et al 1983; YUAN et al 2017). A high plasma concentration of diclofenac is a key pharmacokinetic element to reach synovia. After 6 hours a single intravenous 75mg injection, the diclofenac synovial concentration corresponds to 166% of plasma levels (FOWLER et al. 2017). However, after the first-pass metabolism, approximately only 50% of the drug reaches the systemic circulation in an unchanged form, and this extensive metabolism accounts for diclofenac having poor oral bioavailability (KASPEREK et al 2017). Moreover, after an oral diclofenac intake, large interindividual differences in plasma concentrations were observed (HELLMS et al 2019). These individual variations may

account for therapeutic inefficiency, due to low serum concentrations, and for the observed adverse reactions, when higher serum levels were achieved.

5. Conclusions

Our results demonstrate the anti-arthritic activity of DIC-LNC. Using stereological analysis, we calculated the articular volume of MTP and its components, the surface area of the cartilage and synovium and 2-D cellular count profile of chondrocytes. We demonstrated that the lipid-core nanocapsule reduced the joint synovitis and preserved the articular cartilage, chondrocytes and synovial space. DIC-LNC is a promising nanoformulation for future treatment of RA. However, more analysis needs to be made regarding the effects of nanocapsules in humans.

6. References

ALTMAN, R. et al. Advances in NSAID development: Evolution of diclofenac products using pharmaceutical technology. **Drugs**, v. 75, n. 8, p. 859-877, 2015.

ANDERSON, G. D. et al. Selective inhibition of cyclooxygenase (COX)-2 reverses inflammation and expression of COX-2 and interleukin 6 in rat adjuvant arthritis. **Journal of Clinical Investigation**, v. 97, n. 11, p. 2672–2679, 1 jun. 1996.

ANDERSON, G. D. et al. Combination therapies that inhibit cyclooxygenase-2 and leukotriene synthesis prevent disease in murine collagen induced arthritis. **Inflammation Research**, v. 58, n. 2, p. 109-117, 2009.

ARTACHO-PÉRULA, E. et al. Stereological analysis of the synovial membrane in rheumatic disorders: diagnostic value of volume-weighted mean nuclear volume estimation. **Histopathology**, v. 25, n. 4, p. 357–363, 1 out. 1994.

ASQUITH, D. L. et al. Animal models of rheumatoid arthritis. **European Journal of Immunology**, v. 39, n. 8, p. 2040–2044, 2009.

BADDELEY, A. J.; GUNDERSEN, H. J. G.; CRUZ-ORIVE, L. M. Estimation of surface area from vertical sections. **Journal of Microscopy**, v. 142, n. 3, p. 259–276, 1 jun. 1986.

BECK, R. C. R.; POHLMANN, A. R.; GUTERRES, S. S. Nanoparticle-coated microparticles: Preparation and characterization. **Journal of Microencapsulation**, v. 21, n. 5, p. 499–512, ago. 2004.

BERNARDI, A. et al. THEMED SECTION : MEDIATORS AND RECEPTORS IN THE RESOLUTION OF INFLAMMATION Effects of indomethacin-loaded nanocapsules in

experimental models of inflammation in rats. **British Journal of Pharmacology**, v. 158, n. 4, p. 1104–1111, 2009.

BERNARDI, A. et al. Protective effects of indomethacin-loaded nanocapsules against oxygen-glucose deprivation in organotypic hippocampal slice cultures: Involvement of neuroinflammation. **Neurochemistry International**, v. 57, n. 6, p. 629–636, 1 nov. 2010.

BOECHAT, A. L. et al. Methotrexate-loaded lipid-core nanocapsules are highly effective in the control of inflammation in synovial cells and a chronic arthritis model. **International Journal of Nanomedicine**, v. 10, n. 1, p. 6603–6614, 2015.

BOYCE, R. W. et al. Design-based stereology: introduction to basic concepts and practical approaches for estimation of cell number. **Toxicologic pathology**, v. 38, n. 7, p. 1011-1025, 2010.

BRAND, D. D.; LATHAM, K. A.; ROSLONIEC, E. F. Collagen-induced arthritis. **Nature Protocols**, v. 2, n. 5, p. 1269-1275, 2007.

BULCÃO, R. P. et al. In vivo toxicological evaluation of polymeric nanocapsules after intradermal administration. **European Journal of Pharmaceutics and Biopharmaceutics**, v. 86, n. 2, p. 167–177, fev. 2014.

CAI, X. et al. The comparative study of Sprague-Dawley and Lewis rats in adjuvant-induced arthritis. **Naunyn-Schmiedeberg's Archives of Pharmacology**, v. 373, n. 2, p. 140–147, 2006.

CATTANI, V. B. et al. Lipid-core nanocapsules restrained the indomethacin ethyl ester hydrolysis in the gastrointestinal lumen and wall acting as mucoadhesive reservoirs. **European Journal of Pharmaceutical Sciences**, v. 39, p. 116–124, 2010.

CHAN, F. K. L. et al. Celecoxib versus omeprazole and diclofenac in patients with osteoarthritis and rheumatoid arthritis (CONDOR): A randomised trial. **The Lancet**, v. 376, n. 9736, p. 173–179, 2010.

CHIONG, H. S. et al. Cytoprotective and enhanced anti-inflammatory activities of liposomal piroxicam formulation in lipopolysaccharide-stimulated RAW 264.7 macrophages. **International Journal of Nanomedicine**, v. 8, p. 1245–1255, 2013.

CHOY, E. Understanding the dynamics: Pathways involved in the pathogenesis of rheumatoid arthritis. **Rheumatology (United Kingdom)**, v. 51, n. sup 5, p. 3-11, 2012.

CROFFORD, L. J. Use of NSAIDs in treating patients with arthritis. **Arthritis Research and Therapy**, v. 15, n. sup 3, p. 1-10, 2013.

CRUZ-ORIVE, L. M. Precision of Cavalieri sections and slices with local errors. **Journal of Microscopy**, v. 193, n. 3, p. 182–198, 1999.

CRUZ, L. et al. Physico-chemical characterization and in vivo evaluation of indomethacin ethyl ester-loaded nanocapsules by PCS, TEM, SAXS, interfacial alkaline hydrolysis and

antiedematogenic activity. **Journal of Nanoscience and Nanotechnology.** v. 6, n. 9-10, p. 3154-3162, 2006.

DA SILVEIRA, E. F. et al. Ketoprofen-loaded polymeric nanocapsules selectively inhibit cancer cell growth in vitro and in preclinical model of glioblastoma multiforme. **Investigational New Drugs**, v. 31, p. 1424–1435, 2013.

DAYER, J. M.; CHOY, E. Therapeutic targets in rheumatoid arthritis: the interleukin-6 receptor. **Rheumatology (Oxford, England)**, v. 49, n. 1, p. 15-24, 2010.

DELL'ISOLA, F.; GUARASCIO, M.; HUTTER, K. A variational approach for the deformation of a saturated porous solid. A second-gradient theory extending Terzaghi's effective stress principle. **Archive of Applied Mechanics**, 2000.

DIARRA, D. et al. Dickkopf-1 is a master regulator of joint remodeling. **Nature Medicine**, v. 13, n. 2, p. 156–163, 21 fev. 2007.

DOLATI, S. et al. Utilization of nanoparticle technology in rheumatoid arthritis treatment. **Biomedicine and Pharmacotherapy**, v. 80, p. 30-41, 2016.

EMERY, P. et al. IL-6 receptor inhibition with tocilizumab improves treatment outcomes in patients with rheumatoid arthritis refractory to anti-tumour necrosis factor biologicals : results from a 24-week multicentre randomised placebo-controlled trial. **Annals of the Rheumatic Diseases**, v. 67, n. 11, p. 1516-1523, 2008.

EXNER, H. E. STEREOLOGY AND 3D MICROSCOPY: USEFUL ALTERNATIVES OR COMPETITORS IN THE QUANTITATIVE ANALYSIS OF MICROSTRUCTURES. **Image Analysis & Stereology**, v. 23, n. 2, p. 73–82, 2011.

FC, B. et al. - The PREMIER study: A multicenter, randomized, double-blind clinical trial of. **Arthritis Rheum**, v. 54, p. 26-37, 2006.

FIEL, L. A. et al. Variable temperature multiple light scattering analysis to determine the enthalpic term of a reversible agglomeration in submicrometric colloidal formulations: A quick quantitative comparison of the relative physical stability. **Colloids and Surfaces A: Physicochemical and Engineering Aspects**, v. 431, n. 8, p. 93–104, 20 ago. 2013.

FIRESTEIN, G. S.; MCINNES, I. B. Immunopathogenesis of Rheumatoid Arthritis. **Immunity**, v. 46, n. 2, p. 183-196, 2017.

FOWLER, P. D. et al. Plasma and synovial fluid concentrations of diclofenac sodium and its major hydroxylated metabolites during long-term treatment of rheumatoid arthritis. **European Journal of Clinical Pharmacology**, v. 25, n. 3, p. 389–394, 1983.

FRANK, L. A. et al. Improving drug biological effects by encapsulation into polymeric nanocapsules. **Nanomedicine and Nanobiotechnology**, v. 7, n. 5, p. 623–639, 1 set. 2015.

FROZZA, R. L. et al. Characterization of trans-resveratrol-loaded lipid-core nanocapsules and

tissue distribution studies in rats. **Journal of Biomedical Nanotechnology**, v. 6, n. 6, p. 694-703, 2010.

GHARAGOZLOO, M.; MAJEWSKI, S.; FOLDVARI, M. Therapeutic applications of nanomedicine in autoimmune diseases: From immunosuppression to tolerance induction. **Nanomedicine: Nanotechnology, Biology, and Medicine**, v. 11, n. 4, p. 1003-1018, ,2015.

GILROY, D. W. et al. The effects of cyclooxygenase 2 inhibitors on cartilage erosion and bone loss in a model of Mycobacterium tuberculosis-induced monoarticular arthritis in the rat. **Inflammation**, v. 22, n. 5, p. 509-519, 1998.

GITTER, B. D. et al. Characteristics of human synovial fibroblast activation by IL-1 beta and TNF alpha. **Immunology**, v. 66, p. 196–200, 1989.

GOUVEIA, V. M. et al. Non-biologic nanodelivery therapies for rheumatoid arthritis. **Journal of Biomedical Nanotechnology**, v. 11, n. 10, p. 1701-1721, 2015.

GULATI, M.; FARAH, Z.; MOUYIS, M. Clinical features of rheumatoid arthritis. **Medicine (United Kingdom)**, v. 46, n. 4, p. 211-215, 2018.

GUNDERSEN, H. J. G. et al. Some new, simple and efficient stereological methods and their use in pathological research and diagnosis. **APMIS**, v. 96, p. 379–394, 2009.

GUNDERSEN, H. J. G.; JENSEN, E. B. The efficiency of systematic sampling in stereology and its prediction. **Journal of Microscopy**, v. 147, n. 3, p. 229–263, 1987.

HELLMS, S. et al. Single-dose diclofenac in healthy volunteers can cause decrease in renal perfusion measured by functional magnetic resonance imaging. **Journal of Pharmacy and Pharmacology**, v. 71, n. 8, p. 1262–1270, 2019.

HOBSON, D. W. Nanotechnology. In: **Comprehensive Biotechnology, Second Edition**, 2011.

HOWARD, C. V; REED, M. G. **Unbiased Stereology Three-dimensional Measurement in Microscopy Second Edition**, p. 17, 1998

HUNT, R. H. et al. Myths and facts in the use of anti-inflammatory drugs. **Annals of Medicine**, v. 41, n. 6, p. 423-437, 2009.

JÄGER, E. et al. Sustained release from lipid-core nanocapsules by varying the core viscosity and the particle surface area. **Journal of Biomedical Nanotechnology**, v. 5, n. 1, p. 130–140, fev. 2009.

KASPEREK, R. et al. Pharmacokinetics of diclofenac sodium and papaverine hydrochloride after oral administration of tablets to rabbits. **Acta Poloniae Pharmaceutica - Drug Research**, 2015.

KELLER, K. K. et al. Bone Formation and Resorption Are Both Increased in Experimental Autoimmune Arthritis. **PLoS ONE**, v. 7, n. 12, p. 1–7, 27 dez. 2012.

KELLER, K. K. et al. Improving efficiency in stereology: A study applying the proportionator

and the autodisector on virtual slides. **Journal of Microscopy**, v. 251, n. 1, p. 68–76, 2013.

KOROTKOVA, M.; JAKOBSSON, P. J. **Persisting eicosanoid pathways in rheumatic diseasesNature Reviews Rheumatology**Nature Publishing Group, , 2014.

KRISTENSEN, K. D. et al. Quantitative histological changes of repeated antigen-induced arthritis in the temporomandibular joints of rabbits treated with intra-articular corticosteroid. **Journal of Oral Pathology and Medicine**, v. 37, n. 7, p. 437–444, 2008.

KROENKE, K.; KREBS, E. E.; BAIR, M. J. Pharmacotherapy of chronic pain: a synthesis of recommendations from systematic reviews. **General Hospital Psychiatry**, 2009.

KU, E. C. et al. Effect of diclofenac sodium on the arachidonic acid cascade. **The American Journal of Medicine**, v. 80, n. 4 SUPPL. 2, p. 18–23, 28 abr. 1986.

LANAS, A. Nonsteroidal antiinflammatory drugs and cyclooxygenase inhibition in the gastrointestinal tract: A trip from peptic ulcer to colon cancer. **American Journal of the Medical Sciences**, 2009.

LENG, P. et al. Effects of human cyclooxygenase-2 gene silencing on synovial cells of rheumatoid arthritis mediated by lentivirus. **Artificial Cells, Nanomedicine and Biotechnology**, v. 46, n. sup3, p. S274–S280, 12 nov. 2018.

LI, P.; SCHWARZ, E. M. **The TNF-?? transgenic mouse model of inflammatory arthritisSpringer Seminars in Immunopathology**, 2003.

LOCKWOOD, E. H.; EVES, H. Great Moments in Mathematics (Before 1650). **The Mathematical Gazette**, 2007.

MA, M. H. Y.; KINGSLEY, G. H.; SCOTT, D. L. A systematic comparison of combination DMARD therapy and tumour necrosis inhibitor therapy with methotrexate in patients with early rheumatoid arthritis. **Rheumatology**, 2009.

MCINNES, I. B.; SCHETT, G. **Cytokines in the pathogenesis of rheumatoid arthritisNature Reviews Immunology**, 2007.

NOGUEIRA, E. et al. **Folate-targeted nanoparticles for rheumatoid arthritis therapyNanomedicine: Nanotechnology, Biology, and Medicine**, 2016.

OLIVEIRA, C. P. et al. An algorithm to determine the mechanism of drug distribution in lipid-core nanocapsule formulations. **Soft Matter**, v. 9, n. 4, p. 1141–1150, 2013.

PHAM, C. T. N. Nanotherapeutic approaches for the treatment of rheumatoid arthritis. **Wiley Interdisciplinary Reviews: Nanomedicine and Nanobiotechnology**, 2011.

PRASAD, L. K.; O'MARY, H.; CUI, Z. **Nanomedicine delivers promising treatments for rheumatoid arthritisNanomedicine**, 2015.

RAYCHAUDHURI, S. et al. Five amino acids in three HLA proteins explain most of the

association between MHC and seropositive rheumatoid arthritis. **Nature Genetics**, 2012.

SILVA, M. D. et al. Quantitative analysis of micro-CT imaging and histopathological signatures of experimental arthritis in rats. **Molecular Imaging**, v. 3, n. 4, p. 312–318, 2004.

SMOLEN, J. S. et al. New therapies for treatment of rheumatoid arthritis. **Lancet**, v. 370, p. 1861–1874, 2007.

SMOLEN, J. S.; ALETAHA, D.; MCINNES, I. B. Rheumatoid arthritis. **The Lancet**, v. 388, n. 10055, p. 2023–2038, 2016.

STATKUTE, L.; RUDERMAN, E. M. Novel TNF antagonists for the treatment of rheumatoid arthritis. **Expert Opinion**, v. 19, n. 1, p. 105–115, 2010.

THAKUR, S. et al. Novel drug delivery systems for NSAIDs in management of rheumatoid arthritis: An overview. **Biomedicine and Pharmacotherapy**Elsevier Masson SAS, , 1 out. 2018.

THOTE, T. et al. Localized 3D analysis of cartilage composition and morphology in small animal models of joint degeneration. **Osteoarthritis and Cartilage**, v. 21, n. 8, p. 1132–1141, 2013.

TRELLE, S. et al. Cardiovascular safety of non-steroidal anti-inflammatory drugs: Network meta-analysis. **BMJ**, 2011.

TURK, C. T. S. et al. Formulation and Optimization of Nonionic Surfactants Emulsified Nimesulide-Loaded PLGA-Based Nanoparticles by Design of Experiments. **AAPS PharmSciTech**, v. 15, n. 1, p. 161–176, 2013.

UHLIG, T.; MOE, R. H.; KVIEN, T. K. The Burden of Disease in Rheumatoid Arthritis. **PharmacoEconomics**, v. 32, n. 9, p. 841–851, 2014.

VAN DE LAAR, M. Pain Treatment in Arthritis-Related Pain: Beyond NSAIDs. **The Open Rheumatology Journal**, v. 6, p. 320–330, 2012.

VAN WALSEM, A. et al. Relative benefit-risk comparing diclofenac to other traditional non-steroidal anti-inflammatory drugs and cyclooxygenase-2 inhibitors in patients with osteoarthritis or rheumatoid arthritis: A network meta-analysis. **Arthritis Research and Therapy**, 2015.

VENTURINI, C. G. et al. Formulation of lipid core nanocapsules. **Colloids and Surfaces A: Physicochemical and Engineering Aspects**, v. 375, n. 1–3, p. 200–208, 5 fev. 2011.

WEISSIG, V.; PETTINGER, T. K.; MURDOCK, N. Nanopharmaceuticals (part 1): products on the market. **International journal of nanomedicine**, 2014.

WENG, H. H. et al. Equivalent responses to disease-modifying antirheumatic drugs initiated at any time during the first 15 months after symptom onset in patients with seropositive rheumatoid arthritis. **Journal of Rheumatology**, 2010.

YUAN, J. et al. A pharmacokinetic study of diclofenac sodium in rats. **Biomedical Reports**, v. 7, n. 2, p. 179–182, 1 ago. 2017.

ZHANG, Q. et al. Neutrophil membrane-coated nanoparticles inhibit synovial inflammation and alleviate joint damage in inflammatory arthritis. **Nature Nanotechnology**, 2018.